LBL-7141
UC-34c
TID 4500-R66

Proceedings of the Special Bevalac Research Meetings November 1-3, 1977

NOTICE
PORTIONS OF THIS REPORT ARE ILLEGIBLE. It has been reproduced from the best available copy to permit the broadest possible availability.

CONTENTS

Peripheral Collisions
Doug Greiner 1

Central Collisions
Andres Sandoval 19

Comparison of Models of High Energy Nuclear Collisions
Miklos Gyulassy 74

NOTICE
This report was prepared as an account of work sponsored by the United States Government. Neither the United States nor the United States Department of Energy, nor any of their employees, nor any of their contractors, subcontractors, or their employees, makes any warranty, express or implied, or assumes any legal liability or responsibility for the accuracy, completeness or usefulness of any information, apparatus, product or process disclosed, or represents that its use would not infringe privately owned rights.

Editors

Jeannette Mahoney and Catherine Webb

PERIPHERAL REACTIONS

Doug Greiner

We generally think of peripheral collisions as being collisions involving a small amount of overlap of nuclear matter, but since there's no real way of digitizing what the overlap is, we depend upon the idea of peripheral being as peripheral does. For this we have a lot of clues, a clue being "something that guides through an intricate procedure or maze of difficulties."
Here are the clues we have:

We expect to see	**Projectile Fragmentation** fragments at velocities close to the beam velocity.
We expect to see	**Target Fragmentation** perhaps with no beam fragmentation.
We expect an	**$A^{1/3}$ or Less Target Dependence**
	Small $P_\perp$ and $P_\parallel$ Transfer and, at the lower
energies, what is called	**"Deeply Inelastic" Scattering** ,characterized by a bell-shaped curve, large negative Q-values, etc.

Most measurements to date have been inclusive:

$$P + T \rightarrow F + \text{Anything Else},$$

and therein, perhaps, lies a lot of our difficulty. "Anything Else" implies a whole string of possibilities, including that of large energy and momentum transfer.

Now, how much of the cross section we see looks peripheral? To get an idea of the magnitude of the area that we're looking at:

For ^{16}O at 2.1 GeV/A, the cross section behaves as a peripheral cross section approximately 30% of the time for Pb and 80% of the time for H. It's interesting that hydrogen only gets up to 80%.
As a demonstration of that fact, here is an example of some data taken by Peter Lindstrom.

The upper line is cross section for oxygen breaking up into anything that is not oxygen and the second line going up is the amount of the oxygen that ends up as bound particles moving in the forward direction, i.e., fragments of mass ≥ 2. The third line is the ratio of the bound-particle cross section to the total fragmentation cross section and its value is .8 for hydrogen and .3 for lead.

The cross section for total fragmentation rises and is going up approximately as $A^{2/3}$, so it's rising as the whole area of the target, while this fragmentation cross section is only rising as $A^{1/4}$. The ratio is going from about 80% for hydrogen down to about 30% for lead. The total reaction cross section is only slightly higher than the total fragmentation cross section, so essentially 80% of the cross section behaves as $A^{1/4}$ for a hydrogen target.

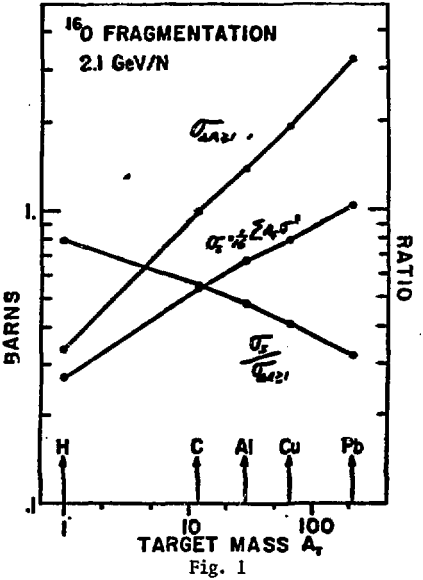

Fig. 1

This is a compilation of the experiments that have been done, the data that's available and some approved experiments that are yet to be done. The references are a partial list of the data that's available and these include measurements done at both the Bevatron and the 88". All of these 1's are by the Chamberlain group which overlap with carbon data from the Heckman/Greiner group, represented by the 2's. The 5 is data taken by the Poskanzer/Gutbrod group. You'll notice that there are few measurements of the heavier beams at any energy.

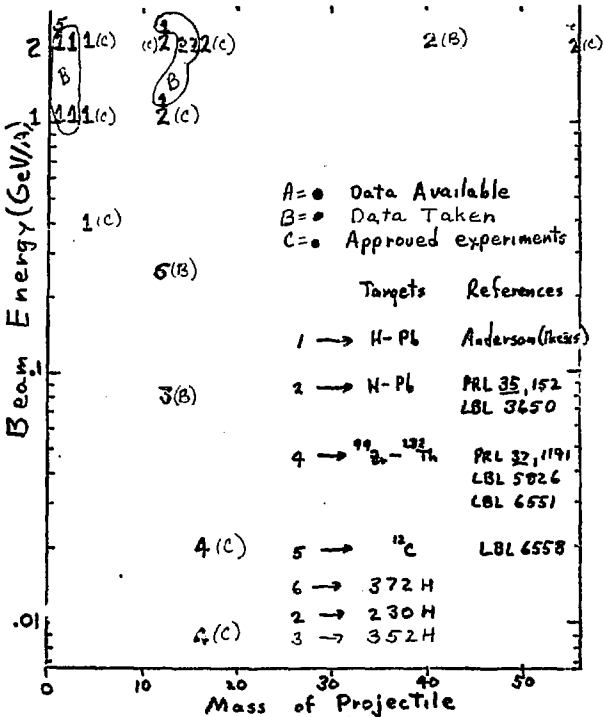

Fig. 2

One of the first general concepts which we found that can be applied to these reactions is **limiting fragmentation**, and the variable of interest is the rapidity variable,

$$y \equiv \tanh^{-1} P_{\parallel}/E$$

and for $P_{\perp} = 0$ $\quad y = \tanh^{-1}\beta$

Some typical values are

ENERGY	Y
2.1	2
1.05	1.4

and a typical fragment distribution is ~.1 to .2 units wide if you're looking at, say, the projectile fragments.

The prediction is that the invariant cross section

$$E d^2\sigma/P^2 dp d\Omega$$

is independent of E in the limiting region, and what determines the limiting region is not predicted, but the idea is that there's a loss of communication between the target and the projectile-like fragments when they're separated by several of units of rapidity. This has been tested at 1 and 2 GeV/A for He, C and O projectiles and it's been found to be valid with some restrictions on the transverse momentum, mainly that the transverse momentum be below .4 GeV/c. Anderson has shown that by 400 MeV/A helium fragmentation is not limiting. If you integrate these cross sections over the momentum distribution and look at their energy dependence they are constant down to 80, even to 20 MeV/A, but definitely change by 9 MeV/A. Although there is no real prediction, if you assume the correlation length is something like the width of the momentum distribution, then you would expect the hypothesis to break down when the target fragments begin to overlap the projectile fragments, which is certainly true at 80 MeV/A.

This is the distribution of fragments from alpha fragmentation at 2.88 GeV/c/A showing the structure of the spectrum in rapidity space. You can see there's a small width peak near the rapidity of the beam and a large valley which is much more pronounced for the heavier particles. For the ^3H and ^3He one can see the beginning of the corresponding peaks for the target fragments. These spectra are typical fragmentation momentum distributions.

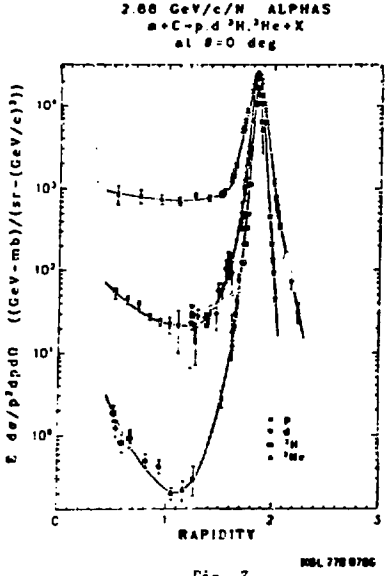

Fig. 3

Looking at the ratio of this fragmentation partial cross section at 80 MeV/A which has been integrated over momentum to an integrated cross section at 2.1 GeV/A, we see that the element cross sections are very much the same and even the ratio of the isotope cross sections remain constant. This is contrary to some of the emulsion data I've seen which says there should be some energy variation before this point. Whether it's fortuitous or not will be seen by looking at other energies. If you'll recall from the other graph there is an experiment which is getting ready to take data at 250 MeV/A.

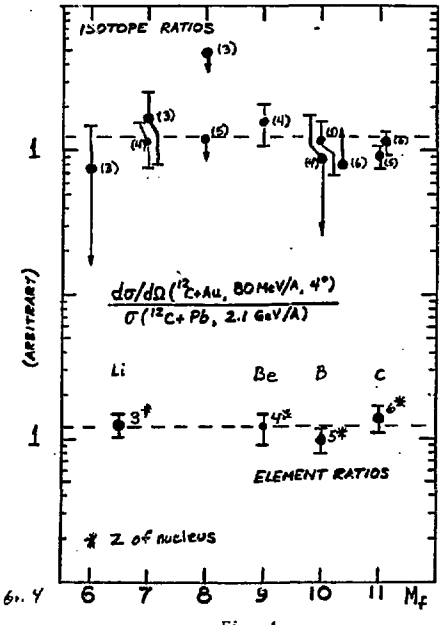

Fig. 4

This data from the 88 compares both element and isotope yields for 20 MeV/A and for 9 MeV/A. For the 20 MeV/A data compared to 2.1 GeV/A, although the isotope points seem to be deviating, the element ratio remains constant. But as soon as you go down to about 9 MeV/A everything changes.

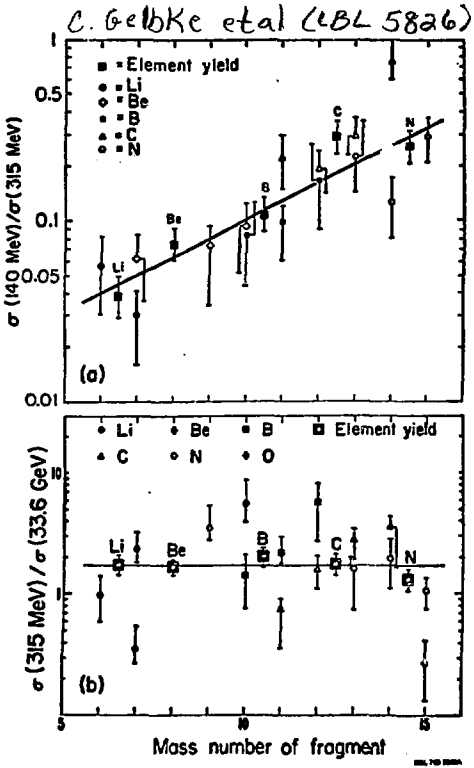

Fig. 5

Another property that can be expected is **factorization**. If the correlation length is small compared to the separation in rapidity space you'd expect the cross section to factor to a term that depends essentially on the geometry of the beam and the target and a term that depends on the beam and the fragment

$$E d\sigma_{PT}/P^2 dp d\Omega = \gamma_{PT}\gamma_{PF} ,$$

again believing that there's no communication between this area and the rapidity space in this area except for geometrical effects. Quite early the cross section was found to factor in this way for carbon and oxygen fragments at 1–2 GeV/A and for oxygen at .02 GeV/A.

It fails in three cases. For heavy targets there are the Coulomb effects.

When you look at single nucleon removal from the beam as you go up in target there's a z^2 target dependence in the cross sections and it's been hypothesized that this is due to the first observation of a collective effect, namely a Coulomb dissociation, and it needs to be verified by seeing both fragments in the same reaction.

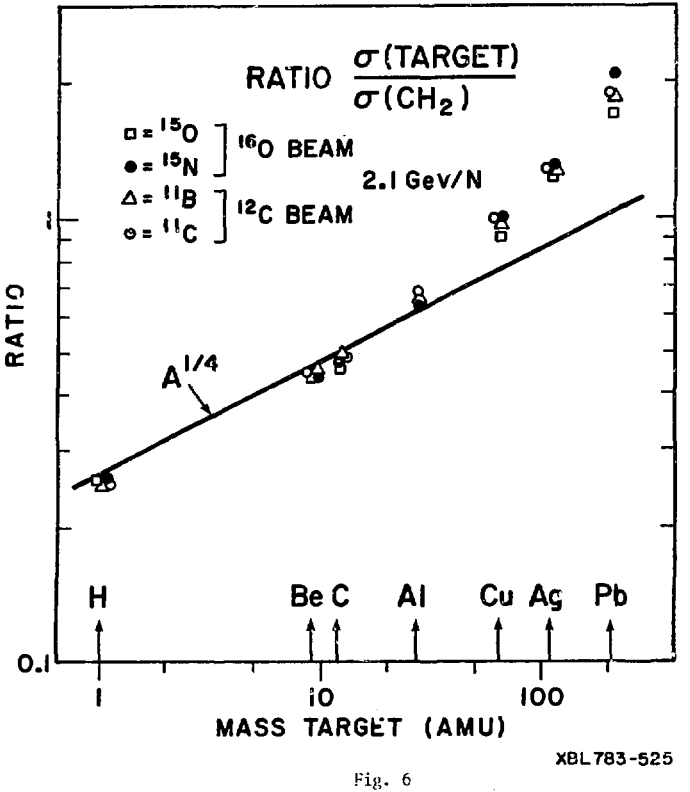

Fig. 6

Another place where this is violated is for light fragments from heavy beams and this is some data in the target rest system taken by Hank Crawford, and between an argon beam and a carbon beam he's looking at the fragments from the same target, gold. The ratio is steadily changing as you go to lower mass fragments. You could still say that factorization may hold at 0 degrees and as we go to higher transverse momentum we're getting more central collisions and deviating from $A^{1/4}$.

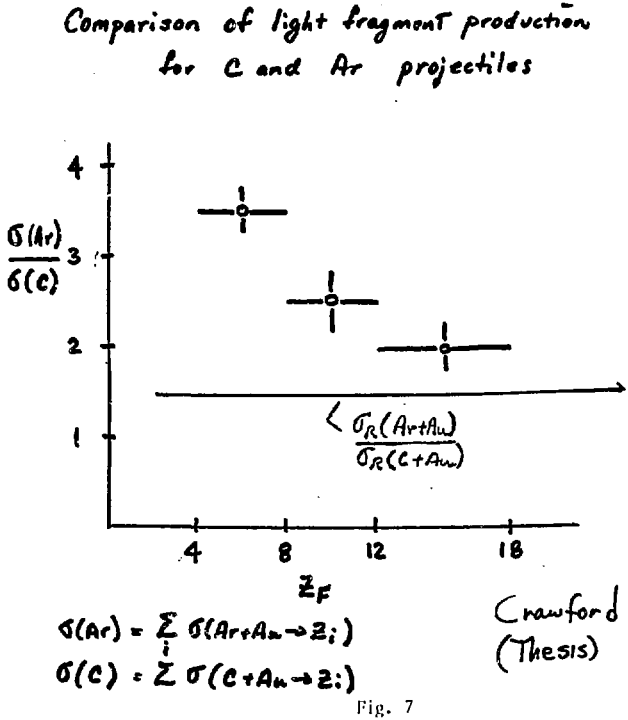

Fig. 7

Another case is between 20 MeV/A and 9 MeV/A. If the cross section factors we would expect these two lines to have the same slope. This is a target mass difference of 94 to 208. Again, somewhere between 20 MeV/A and 9 MeV/A there is a change, so it would be interesting to see the energies in between.

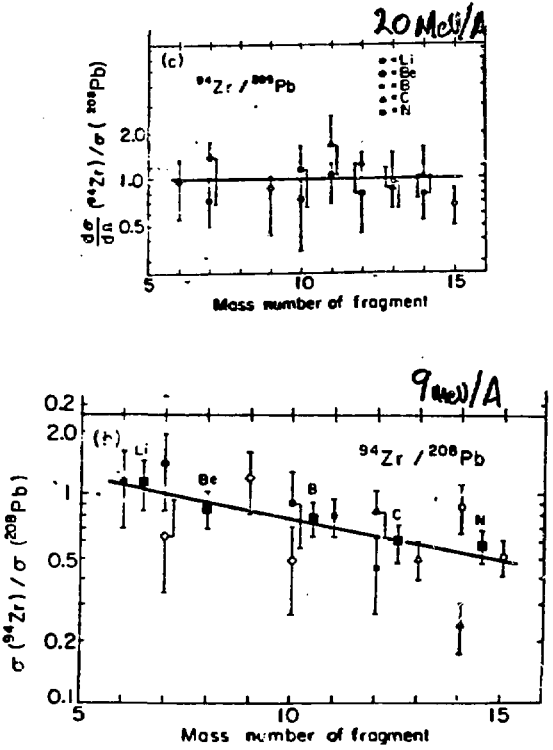

Fig. 8

There are many models with which to look at these fragmentation cross sections, which I won't go into now. In general they give poor fits and since fitting these cross sections is a hard problem, I think this is a good time to find a way to quantify the fits of the models. For example, Lukyanov has a model where he assumes an excitation parameter giving the temperature, T, another parameter for the deviation of momentum distribution from parabolic shape, and a normalization parameter. So that's three parameters for each charge, with 3–4 isotopes/charge, and you can do a fit to the isotopes of a given charge. If we define

$$\text{goodness-of-fit} \equiv \frac{\Sigma(\text{theory}-\text{exp.})^2/\sigma^2}{\text{NDF}}$$

where *NDF* is the number of degrees of freedom, we get

$$1.8_{(\text{Li})} \leq \chi^2/\text{NDF} \leq 296_{(\text{He})},$$

which is a very good fit for Li ranging out to a very poor one for He, with an average χ^2 of 75. It's an excellent model for looking at systematics between isotopes and for getting an idea of what the temperature is. But the temperature does vary — for the charge 8 particles it's about 4 MeV; for the charge 1, it's about 13. I think the conclusion is that the χ^2 test is too hard on the models. So we should invent a Better Statistic, and I propose

$$\text{BS} = \Sigma\ \text{maxof}(\ |\text{exp/model}|\ ,\ |\text{model/exp}|\ ) - 1/\text{NDF}$$

which has the advantages that it is independent of experimental errors, and therefore the model will not be hurt by good experiments, and it measures the ratio of theory to experiment. And when people talk about models they talk about the model being good within a factor of 2 or a factor of 10. We can quantify it by the Better Statistic. So a perfect theory would have

$$\text{BS} = 0$$

and a factor of 2 theory, $\text{BS} = 1.$

So here is a short look at some of the models.

This Silberberg and Tsao model is strictly an empirical model and we're estimating that they put in 15 parameters, so they have a BS value of 2.5. Lukyanov doesn't fare too well. He has too many free parameters. With the abrasion-ablation model Hüfner has zero free parameters and he's doing better than anyone else. It's interesting to note that if you just say that if a fragment comes out it just depends on how tightly bound that fragment is, which is essentially just an exponential fit to the fragmentation part of the cross section.

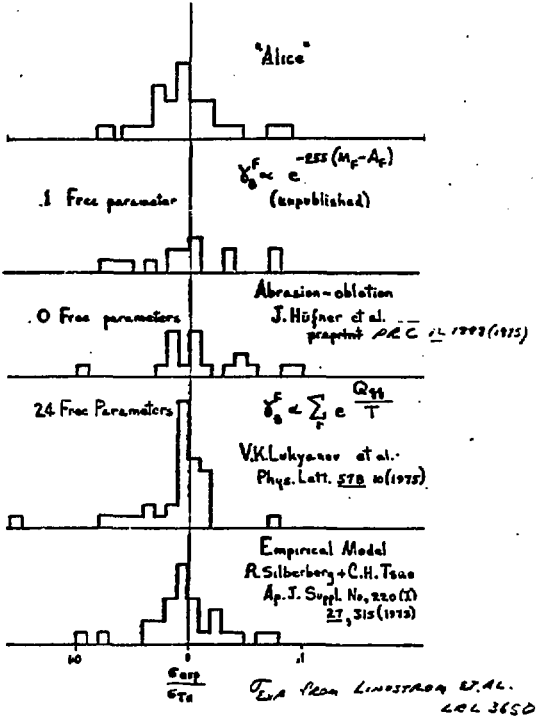

Fig. 9

Fragment Momentum Distributions

1. For heavy fragments out to about 400 MeV/c they are generally Gaussian.

2. They're centered slightly below beam momentum.

3. They have tails when you go down about a decade or so in flux, and they've been interpreted as the temperature.

The first two properties can be derived rather simply by assuming an excitation and conservation of momentum, and they also follow from the impulse approximation. However, there is no valid prediction of the momentum distribution widths by any model. There is the parabola shape with which you're all familiar which exhibits the general trend but there are major deviations from that.

Most models predict isotropy and it's certainly not true for the lighter fragments and for heavier fragments it's only been verified to about the 10% level and that's only where the cross section is still roughly 1 or 2 decades below the peak. The ^{4}He fragment distributions are definitely not isotropic.

This is a contour plot of rapidity vs transverse momentum for protons coming from a helium reaction with carbon and you can see it's almost isotropic, but you still have tails coming off toward the target region of rapidity. The scale is normalized so that isotropy is indicated by a circular contour at low $p_\perp$ and $p_\parallel$. At large $p_\perp$ and $p_\parallel$ we see the anisotropy of the distributions.

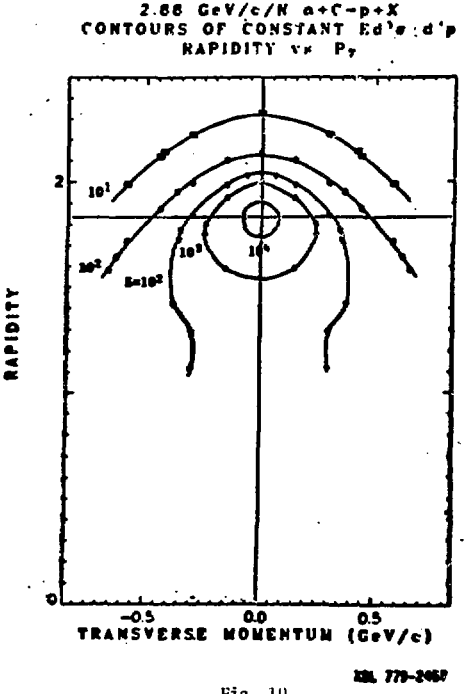

Fig. 10

This is data of target fragments from protons on carbon from the Poskanzer/Gutbrod group. The dashed curves show the transformation to the lab energy frame of the Gaussian momentum distributions seen at 2.1 GeV/A. The tails of the distributions clearly deviate, indicating a different process is responsible for the higher momentum fragments.

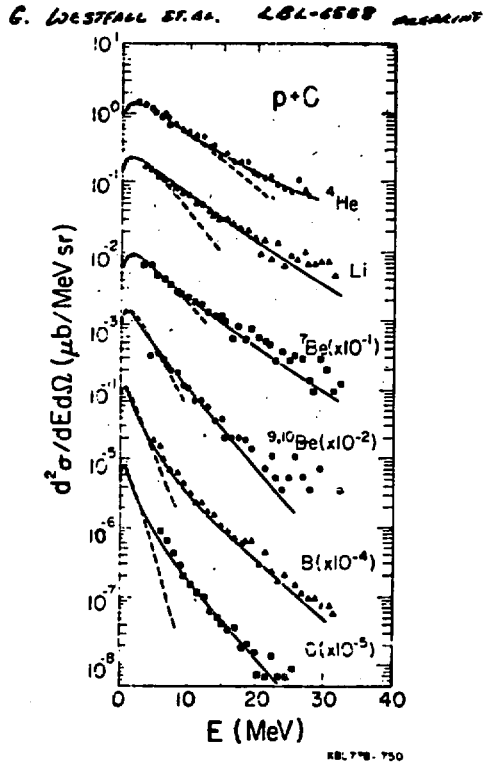

Fig. 11

Future Directions

At the Bevalac we have:

high A and high β

To justify this expensive endeavor we must find:

Fundamental physics results which are *uniquely* available from high A and β.

Otherwise, down the tube.

Our main difficulty is:

high multiplicity of final states

Possible Areas:

1. Nuclear force in the presence of nuclear matter not in equilibrium (is it like N–N?)
2. Effects of known forces on a strongly interacting system.
   i.e., electromagnetic can give a known excitation spectrum.
3. Condensation of excited nuclear matter.
4. Nuclear equation of state.
5. Energy transfer between blobs of nuclear matter.
   i.e., is it different from free nucleons? Are there collective effects?
6. Formation of heavy fragments
   i.e., fast or slow, one or two step
7. Knock on spectrum of nucleons and nuclei by passing nuclear matter.
8. Exotic states (what is their signature?)

How do we look in these areas?

The best way is to define the whole systems (4π exclusive).

This is impossible!

Can we isolate fundamental physics by defining part of the system? How small a part is sufficient?

Single particle inclusive

Results are not conclusive,
models come close with only conservation of P and E,
there is too much integration and interaction.

Consider multiparticle inclusive

Case b~0: maximum interaction of system, impossible to define whole final state.

What is the consequence of the lack of definition?

Will we again see phase space?

Case b≠0: SPI reactions have shown that we have factorization of the strong force and limiting fragmentation.
i.e., independent of the target.

Basic philosophy is: PROJECTILE FRAGMENTATION EXCLUSIVE MEASUREMENTS ALLOW US TO APPLY THE STRONG FORCE IN A CONTROLLED MANNER AND DEFINE THE FINAL STATE SYSTEM.
The final state can be defined because it occupies the forward angles in the laboratory.

I believe this approach allows theoretical tools to be considered.
Perhaps OPEP, sudden approximation, QED.

This approach should yield information in areas 1–3, 5–7.

4 may enter if the models are applied to the forward and backward directions and if they differ.

8 – Who knows? Experiments of this type are:

230,231,350	H/G exclusive measurement with emphasis on projectile fragments
178	Kirk – 2 body clusters
352	Hendrie/Scott, 2 particle projectile fragment correlation.

and HISS

CENTRAL COLLISIONS

Andres Sandoval

In this talk I want to present the experimental status on central collisions; to extract as model-independantly as possible the main trends and conclusions from the data, to present a broad overview, not only the highlights, and to understand aspects of it.

Central collisions are defined as non peripheral collisions, i.e., collisions involving a large projectile and target density overlap. The problems with central collisions are the following:

-There is not one single reaction mechanism, since there are participants and spectators of the primary interaction.

-It often can be very difficult to disentangle both contributions; for example, here one can see the overlap of the two contributions when the cross section from argon on lead is plotted against the rapidity.

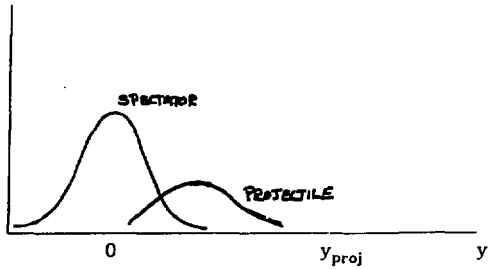

-There is a continuum of impact parameters from really central to *semiperipheral*.

-The non-zero impact parameters will have an inherent asymmetry over which in general the experiment will average.

-It might be that for a *fixed impact parameter* abnormal effects such as high density, pion condensation, etc. have only a small partial amplitude. In order to occur they may require, for example, the instantaneous alignment of the Fermi motion of projectile and target nucleons.

In general, central collision data will be averaged over

internal Fermi motion
impact parameter
azimuthal asymmetry for non-zero impact parameter
participant and spectator contributions.

In spite of the problems, there has been a lot of experimental work on central collisions, which I have listed below. I have attempted to include all of the work and hope I haven't left any out.

	Experiment	Proj	E(MeV/A)	Target	Fragment
1	Nagamiya	C	800	C	π 50-1000 MeV
				Pb	p 50-2000 MeV
		Ne	800	NaF	d, t, ^{3}He, α — single particle; inclusive; associated multiplicity; 2 particle inclusive
				Cu	
				Pb	
2	Nakai	Ne	800	NaF	π^+ 20-100 MeV
				Cu	single particle inclusive
				Pb	associated multiplicity
3	Cork	Ar	400	U	π cross section for multi-pion
			900	U	events
4	Poskanzer/ Gutbrod	He	400	U	p 20-140 MeV/A,
		Ne	250	U	d 20-140 MeV/A, single particle
			400	U	t 20-140 MeV/A, associated multiplicity
			2100	U*	^{3}He 20-140 MeV/A,
			2100	Al	α 20-140 MeV/A

*Li-O 10-60 MeV/A

	Experiment	Proj	E(MeV/A)	Target	Fragment
5	Poskanzer/ Gutbrod	Ar	400	Ca	π^+ 20-100 MeV
				U	p 5-200 MeV
			1050	Ca	d 10-250 MeV
				U	t 10-300 MeV
		Ne	250	U	single particle inclusive
			400	Al	
				U	with associated multiplicity
			1050	U	
		He	400	U	
				Al	
			1050	U	
		p	1040	U	
6	Igo/ Perez Mendez	C	2100	Be	(π) from projectile rapidity
				Cu	p down to intermediate rapidity
		Ar	1800	Be	d single particle inclusive
				Cu	t associated multiplicity
					2 particle inclusive

	Experiment	Proj	E(MeV/A)	Target	Fragment
7	Anderson	p d α C	400 1050 2100	H C Cu Pb	(π) $0.25 \leq P/Z \leq 9$ GeV/c p $0° \leq \theta \leq 12°$ d t projectile fragmentation ^{3}He single particle inclusive α
8	Schroeder	p α	2100 1050	C Cu Pb	π 180° production p single particle inclusive d
9	Price	C Ne Ar	2100	Au U	Li → Na 10-50 MeV/A single particle inclusive
10	Poe	C Ar	400 1050 2100	LiH NaF BaI_2 Pb_3O_4	charged particle exclusive 4π detector π^- multiplicities

	Experiment	Proj	E(MeV/A)	Target	Fragment
11	Heckman/ Greiner	He O Ar	2100 2100 1800	emulsion	black, gray, fast particles 4π detectors correlations analysis
12	Jacquot Strasbourg	O	2100	emulsion	black, gray, fast particles 4π exclusive correlations analysis
13	Schopper	He C O	870 2100 4000 250 1700 4200 870 2100	AgCl	4π detector Angular distributions of prongs in star events

LBL-11220

Biological and Medical Research with Accelerated Heavy Ions at the Bevalac, 1977-1980

M. C. Pirruccello and C. A. Tobias, Editors

DISCLAIMER

Biology and Medicine Division
Lawrence Berkeley Laboratory
University of California
Berkeley, California 94720

This work was supported by the Office of Health and Environmental Research of the U.S. Department of Energy under Contract W-7405-ENG-48.

18	Seaborg Loveland	C	2100	Au Pb U	radiochemical determination of residual nuclei
19	Meyer/ Gutbrod	p α Ne	2100 1050 400	U Au Ag	heavy particles and fission products angular correlations and associated multiplicity

I will now go through these experiments looking at the following experimental observables:

1. Single particle inclusive spectra
   a) π
   b) p
   c) light fragments ($d \rightarrow \alpha$)
   d) not-so-light fragments (Li →)
   e) residual nuclei
   f) fission channel (for intermediate and heavy targets.)

2. Integrated cross sections

3. Charged particle multiplicities
   a) pion multiplicity
   b) unbiased multiplicity
   c) associated multiplicity

4. Multiplicity bias on single particle spectra (by selecting on multiplicities)

5. Correlations

This is Nakai and Chiba's work where we see some peaking at backward angles at about 40 to 60 MeV. The solid lines are the data of Cochran for p–nucleus pion production, which has been scaled according to the z and neutron number of the projectile. $d^2\sigma = Z_{proj}\, d^2\sigma_{p+A\to\pi^+} + N_{proj}\, d^2\sigma_{n+A\to\pi^+}$

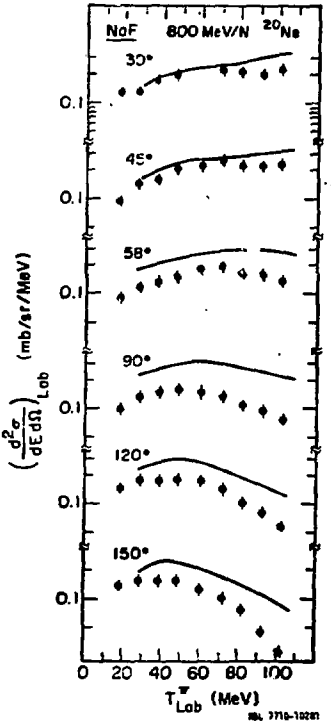

Fig. 1

This is the same data for a heavy target, in this case lead, showing the same features, with the spectra peaking at backward angles, again compared with the scaled up proton–nucleus data.

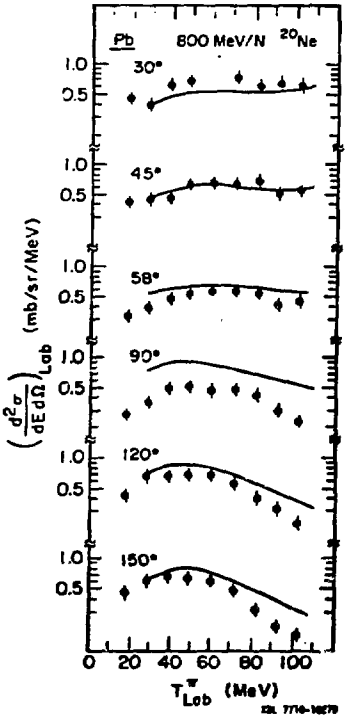

Fig. 2

Here they have transformed their data for the equal projectile and target masses to a center of mass system that is well defined for the equal projectile and target masses and have plotted the angular distributions in the center of mass frame for the different energies. In the center of mass, the angular distributions are symmetric around 90 degrees, so we will have at the high pion energies a forward and backward peaking, while at the lower energies the angular distributions become isotropic or even somewhat peaked at 90 degrees.

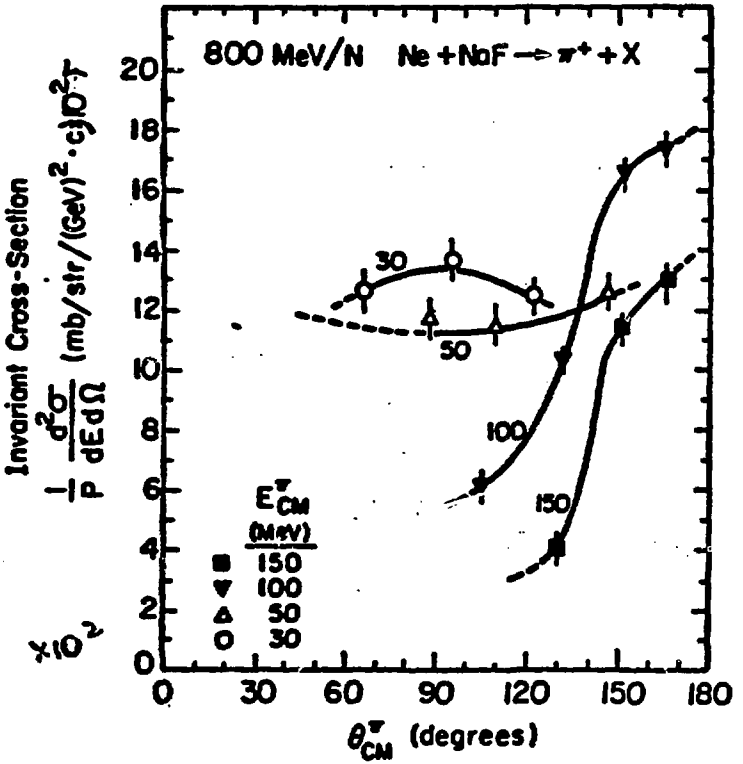

Fig. 3

Higher energy pions have been measured by Nagamiya and here is an example of the same reaction, Ne on NaF, producing π^- from 180 MeV to 1 GeV. The spectra are smooth, exponentially decaying.

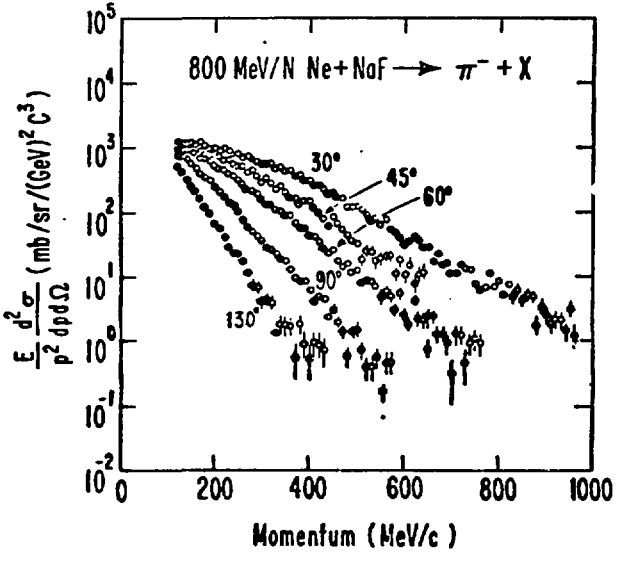

Fig. 4

Here is the same data in a contour plot in rapidity vs $P_\perp$ of the pions with contour lines of constant invariant cross section. They are compared here to an isotropic distribution in the center of mass. For the higher energy pions the lines of constant cross section are very similar in shape to the isotropic distribution in the center of mass, but there is no prediction as to what the slope should be. We see also that the π^+ and π^- yields are the same for equal mass of projectile and target. For the intermediate energies, which also overlap with Nakai's data, they are much broader, having a forward and backward peaking.

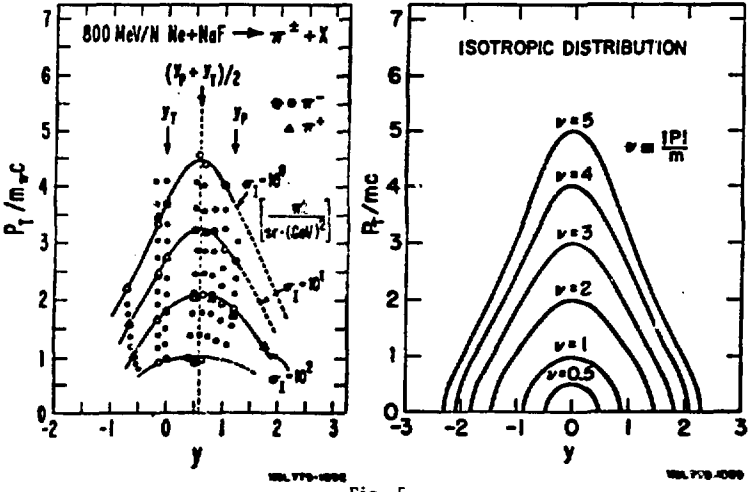

Fig. 5

Plotting the spectra as a function of transverse kinetic energy at half the target and projectile rapidity, we obtain a nice exponential with a characteristic temperature of 55 MeV for equal projectile and target and up to 59 MeV for Ne on Pb.

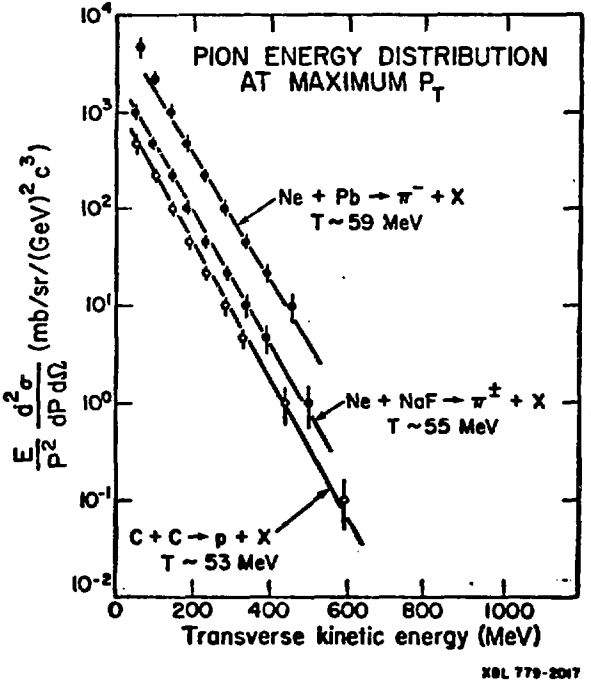

Fig. 6

There are also some data from Lee Schroeder of pion production from protons on lead at 180 degrees. An exponentially decaying spectrum with a slope of about 44 MeV.

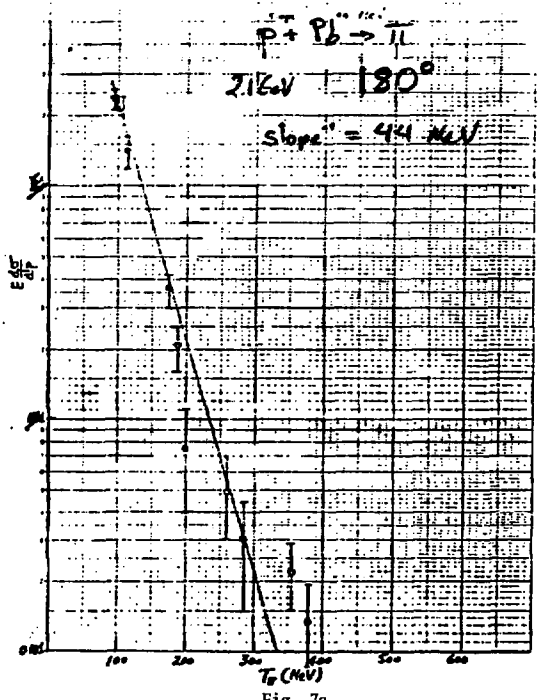

Fig. 7a

Compared here are the π^- production for C + C and Ne + Pb. The main features are the same, suggesting a common origin, e.g., statistical, independent nucleon–nucleon interactions. There are some slight deviations, namely the asymmetry for Ne + Pb. At the present it isn't clear if this is due to some pions from thermal origin, or to absorption and degradation of the pions in the target spectators.

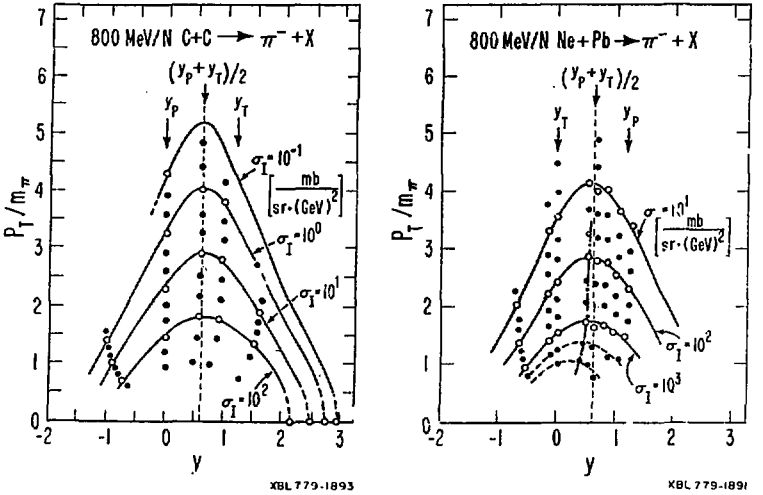

Fig. 7b

Summary of π Data:

a) For C on C and C on Pb the double differential cross sections can be superimposed. (1)

b) For high $p_\perp$ the π production is isotropic in the center of mass. (Ne + NaF)

c) At lower energies, corresponding to the decay energy of the Δ they are forward and backward peaked. Reasonable agreement to p+A data. (1,2)

d) For $E_{cm} < 50$ MeV they are again isotropic in the center of mass. (2)

e) The ion temperature ~ 50 MeV.

f) For equal projectile and target π^+ and π^- have the same yield. (2)

Proton Production

This is proton data from the same reaction, Ne on NaF from Nagamiya's data, looking at protons from 15 to 130 degrees in momentum vs invariant cross section. You see here that the data extends much farther than the beam momenta.

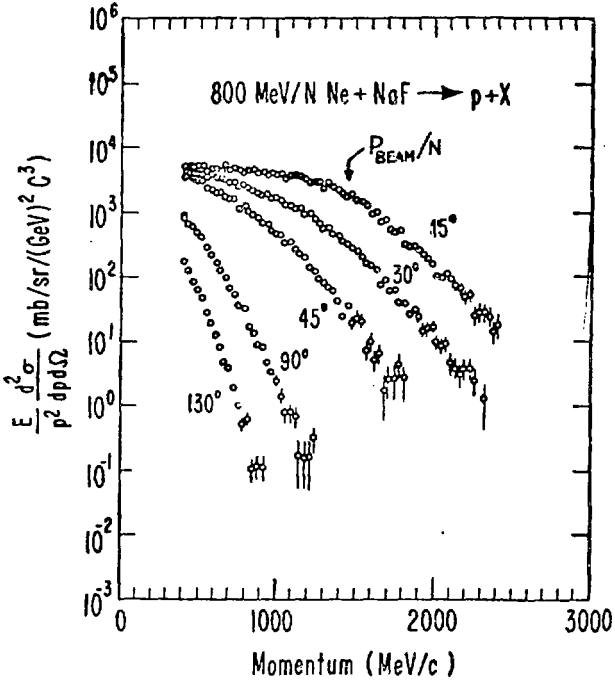

XBL 779-1879

Fig. 8

This is the same data transformed into a $P_\perp$ vs rapidity distribution compared to an isotropic distribution. As expected, it is symmetric about $(y_p+y_t)/2$ but the shape of the lines of constant invariant cross section don't agree with a single isotropic source in the center of mass. For very low $p_\perp$ we actually expect them to peak at the target and projectile rapidities.

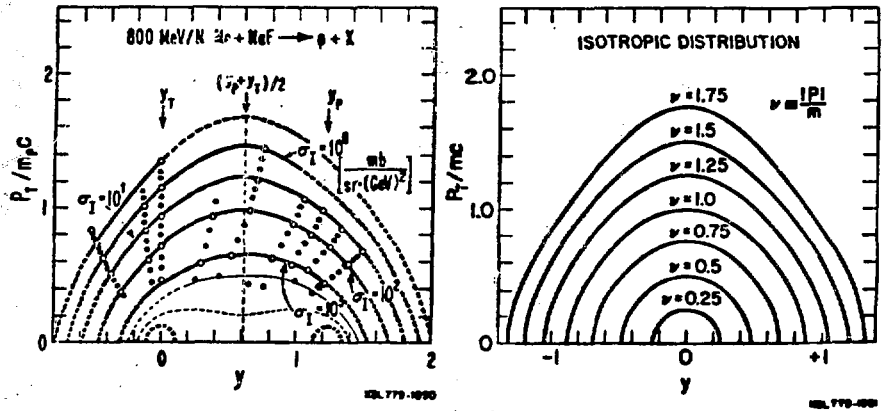

Fig. 9

As we change the mass of the target we get some distortions around the symmetry axis. As the mass of the target increases we lose the symmetry around the intermediate rapidity, as we see here for a lead target. We have a systematic trend in that the maximum of the invariant cross section at a given value of $p_\perp$ occurs at increasing values of the rapidity for increasing $p_\perp$.

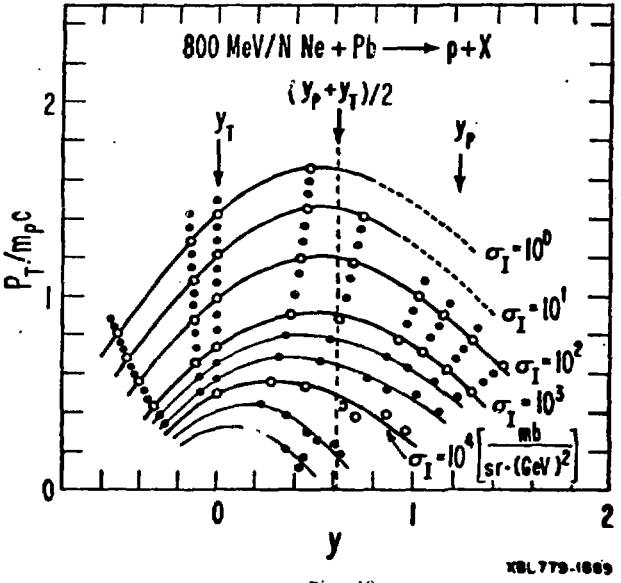

Fig. 10

11

Plotting the spectra along the line of maximum $p_\perp$ for a given level of cross section vs. the transverse energy, they get again nice straight lines with a temperature of the order of 70 MeV.

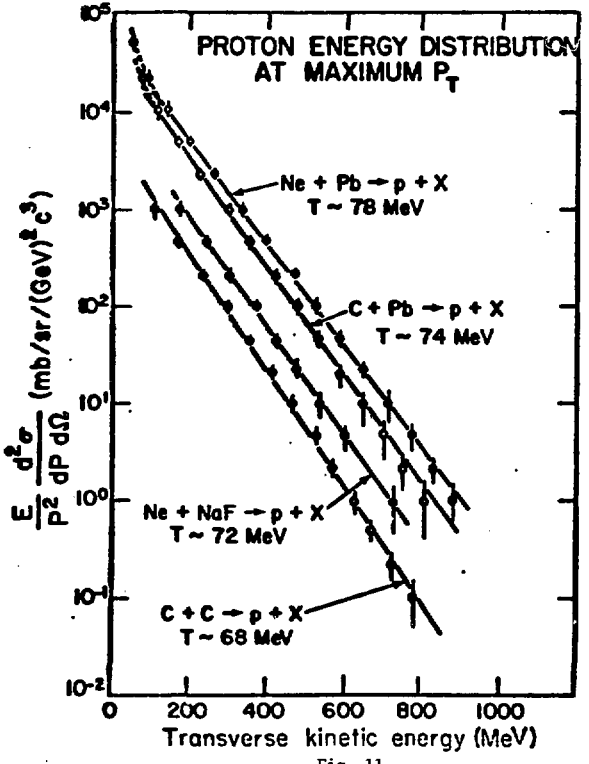

Fig. 11

Here we have proton data for different bombarding energies of Ne and α's on U treated with the fireball model which gives temperatures of from 28 to 47 MeV. At 2.1 GeV/A we were unable to fit the data with the simple fireball model; however, although the absolute normalization of the data is somewhat uncertain, some firestreak model calculations of Jean Gosset, Joe Kapusta and Gary Westfall seem to reproduce the shape fairly well.

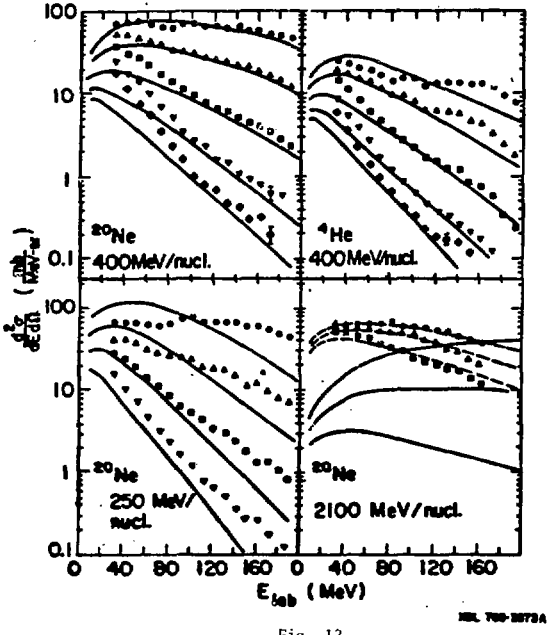

Fig. 12

Here are the contour plots in the $p_\perp$ vs rapidity plane for protons and heavier fragments from Ne+U at 400 MeV/A. We see that there is not a unique source.

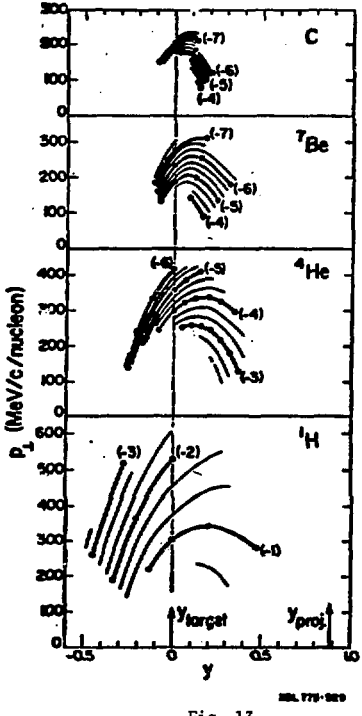

Fig. 13

The proton spectra, as well as the light fragments, show a characteristic saturation effect with the bombarding energy, as shown on this plot of ^{3}He production, namely that the forward production is saturated for different bombardment energies from 250 to 2100 MeV/A, while the higher energies contribute to higher transverse momentum production.

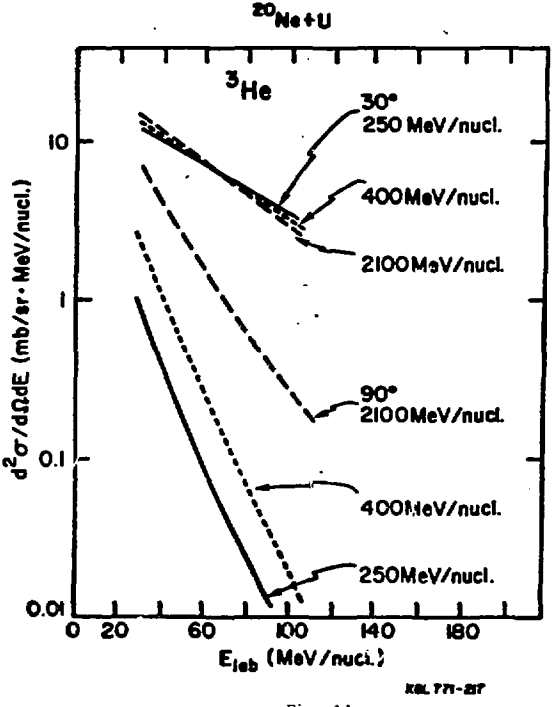

Fig. 14

Summary of p data:

a) non–isotropic in any frame (there isn't a single source) (1, 4, 5)

b) As the bombarding energy increases the yields at forward angles saturate and more $p_\perp$ is produced. (4)

c) At 250 MeV/A and 400 MeV/A bombarding energy they are fit by the fireball model, $\tau =$ 28 MeV– 47 MeV. (4)

d) At 800 MeV/A their temperature, $\tau \sim$ 75 MeV, is higher than the pion temperature. (5)

Light Particle Production:

These light particle production cross sections from Ne on U at 250 MeV/A show the same characteristic features for all fragments – smooth energy spectra, decaying exponentially, and sharply peaked angular distributions.

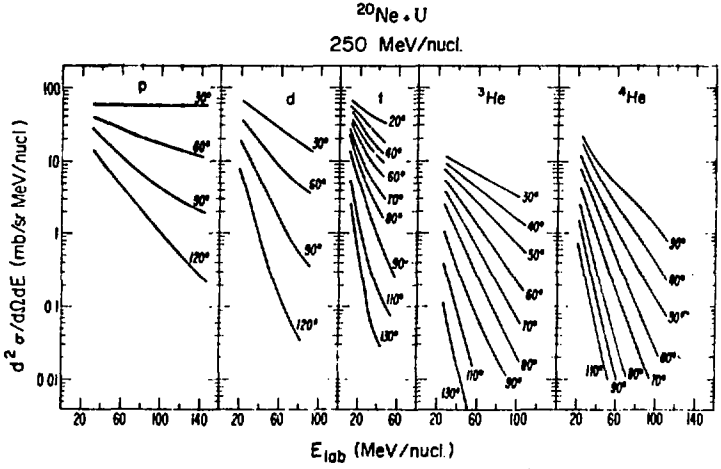

$$d^2\sigma_A = \frac{1}{A!}\left(\frac{4\pi p_0^3 \gamma}{3\sigma_0}\right)^{A-1}\left(d^2\sigma_p\right)^A$$

Fig. 15

These ^{3}He production data in a $P_\perp$ vs rapidity plot are compared at different Ne bombarding energies. You see the beam rapidity moving out and at the same time there is a component of this cross section moving out with with the beam . Again we see that there isn't a unique source.

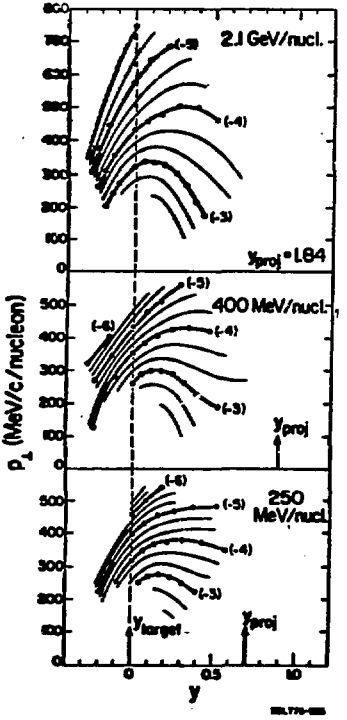

Fig. 16

All these data have been fit with the coalescence model, which takes the proton double differential cross section and scales it to a power corresponding to the fragment mass. It's a remarkably good fit, although there is not much insight into why this is happening.

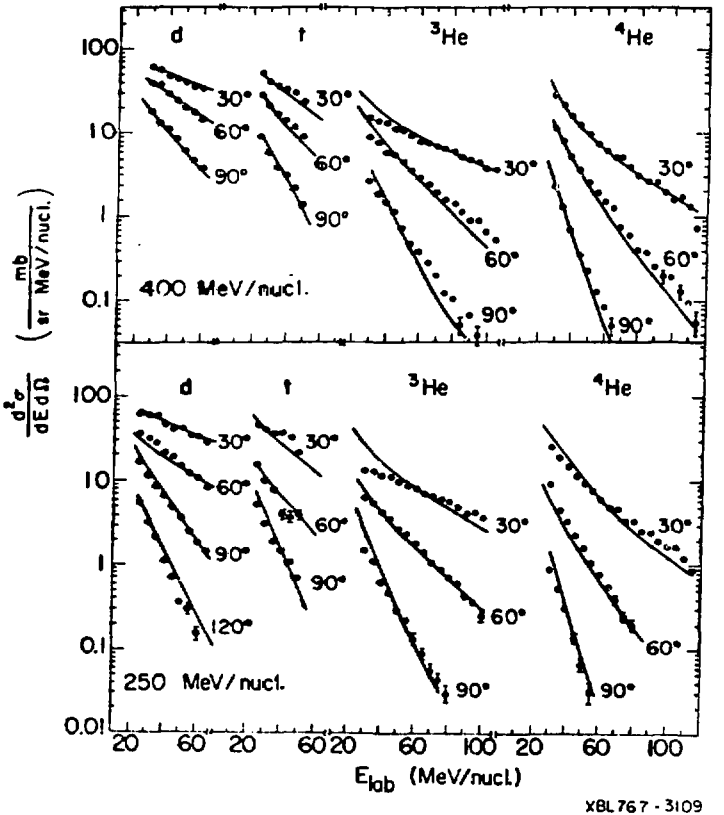

Fig. 17

This can be extended to the heavier fragments also, in this case Li and Be. Again a coalescence fit with a parameter p_0 of around 130 MeV/c. The striking thing is that this model seems to apply also to Anderson's data for the projectile fragmentation, so there might be more physics than the model seems to imply.

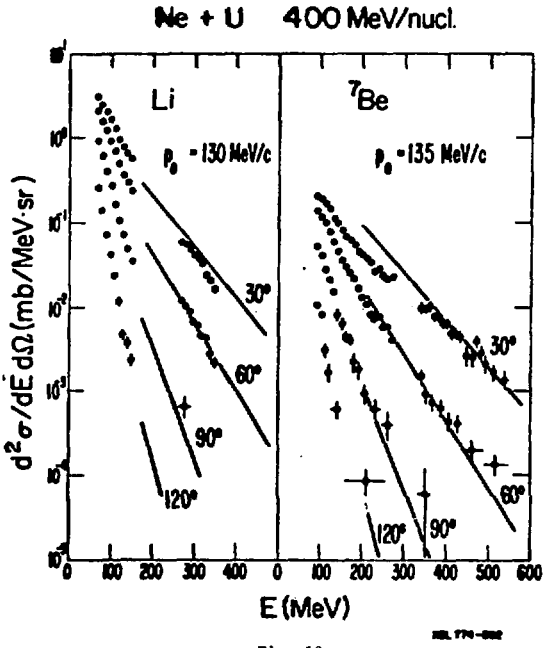

Fig. 18

Jim Carrol's data for d production from Ar+Cu at 1.8 GeV/A. Although the main data is near the projectile rapidity there are some tails that extend down to intermediate rapidities. The solid lines are firestreak model fits to the data. This model divides the projectile and target densities into strips and lets them interact, assuming that for each pair that interact a thermalized system is created. Chemical equilibrium is assumed among the different species. Each firestreak expands to a freezeout density, ρ_0, at which the double differential spectra of all the species are calculated.

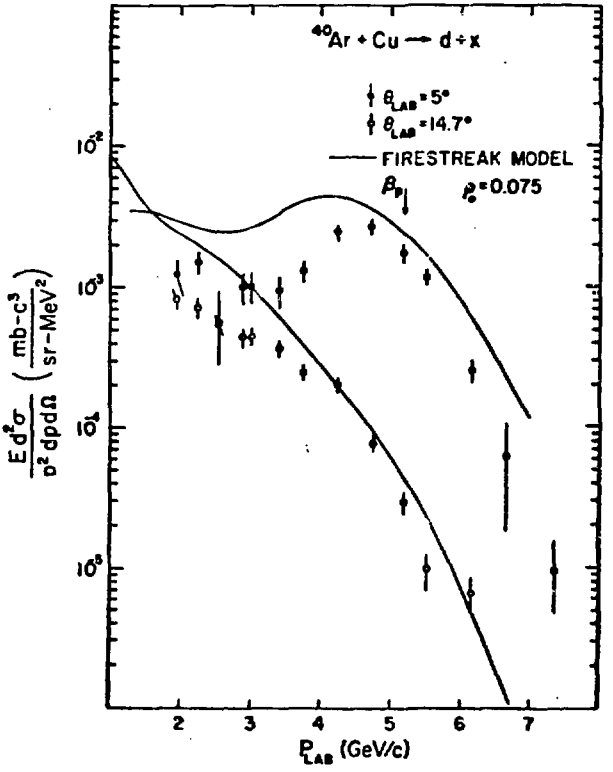

Fig. 19

Again a firestreak fit to the triton data for the same reaction.

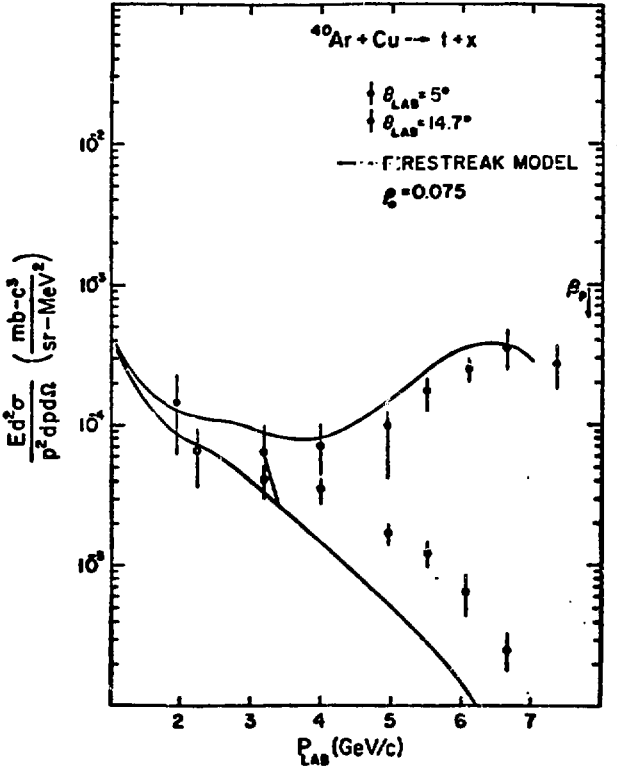

Fig. 20

Summary of light particle production:

Astonishing functional dependence on the proton double differential cross sections. (4,6,9)

$$d^2\sigma_A/P^2dpd\Omega = 1/A!\,(k^{A-1})(d^2\sigma_p/P^2dpd\Omega)^A$$

Integrated Cross Sections

Several groups have integrated the double differential cross sections to extract the dependence of the fragment production on the projectile, target or bombarding energy. Here we have, for example, the π^- production from 800 MeV/A Ne on different targets as a function of the lab angle.

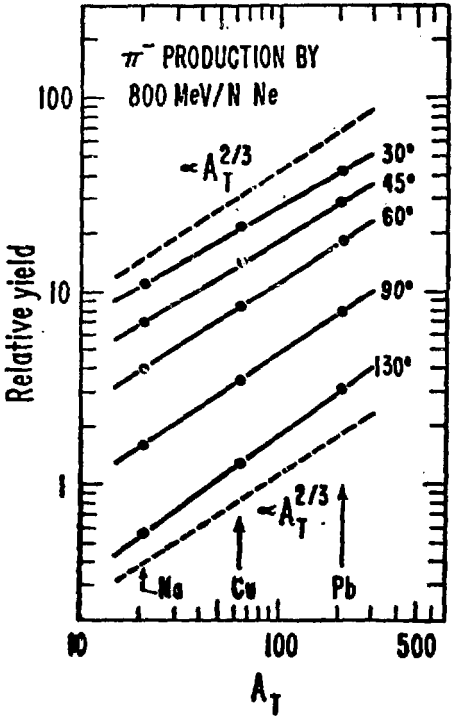

Fig. 21

Here we see the same for the proton production and we have the problem that although the yield gives a straight line as a function of the target mass, its slope changes with angle. This is due to the fact that we are dealing with exponentially decaying spectra which were integrated in an arbitrary energy or momentum bite in the laboratory, so the kinematics has a very strong influence. Also, the participant and spectator contributions change in the different regions and we can't disentangle them.

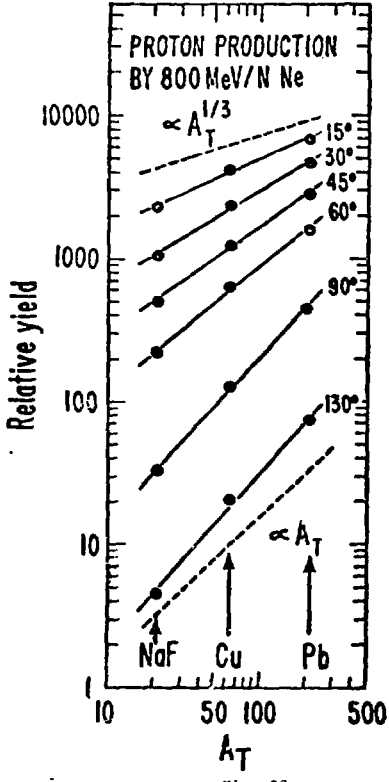

Fig. 22

Summary of Integrated Cross Sections:

It is of no use to compare different projectile, energy, or target combinations. (1, 3, 4, 11, 13)

They are integrated between some arbitrary values and for exponentially decaying spectra the result is strongly dependent on the kinematics.

Multiplicity

This is data from the streamer chamber showing the total multiplicity dependence on the pulse height from the trigger scintillator, a measure of the amount of forward emitted particles from the interaction. Triggering scintillators were placed in front of and behind the target to discriminate against beam particles going through without interacting. We see a very strong dependence, with the very low pulse heights having the highest multiplicities, and corresponding to the more central collisions. This shows one of the problems in defining where the central collisions are.

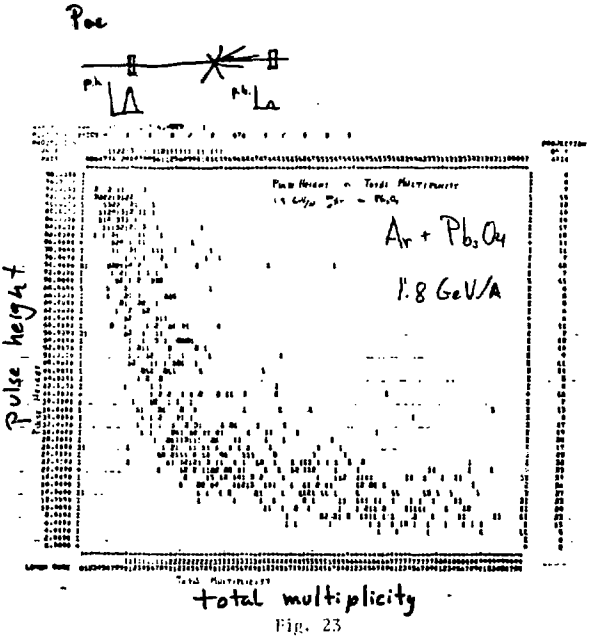

Fig. 23

Here we are looking at the dependence of the total charge multiplicity to the π^- multiplicity and the pion multiplicity is essentially a straight line at about 10% of the total multiplicity. This is from the reaction on lead oxide of Ar at 1.8 GeV/A.

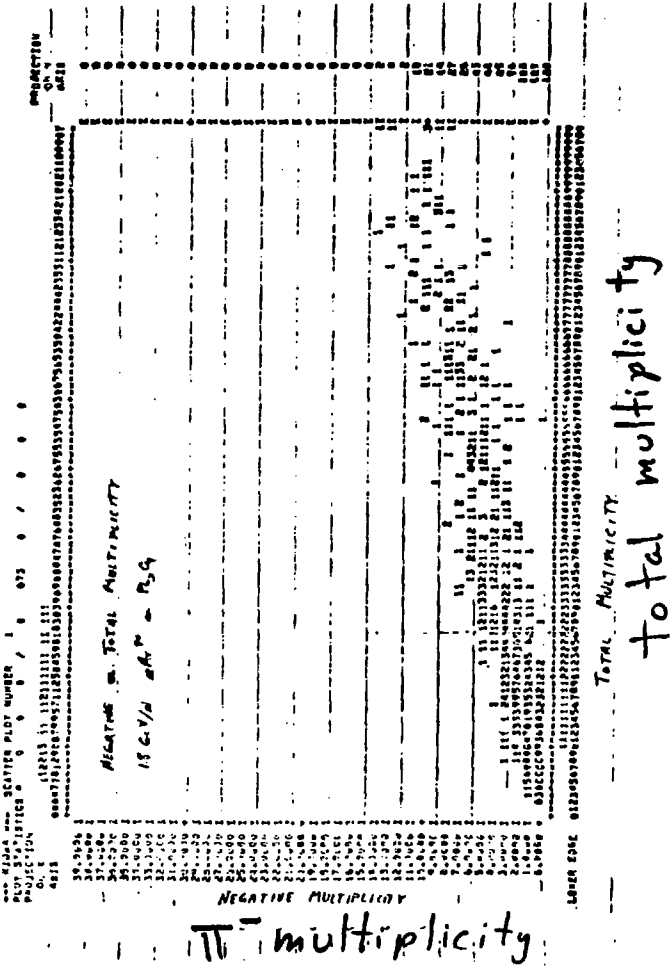

Fig. 24

From the same reaction this is the total multiplicity distribution on a linear scale going from 0 up to 100 charged particles. This is an exponential distribution with the cut-off at lower multiplicities caused by the apparatus.

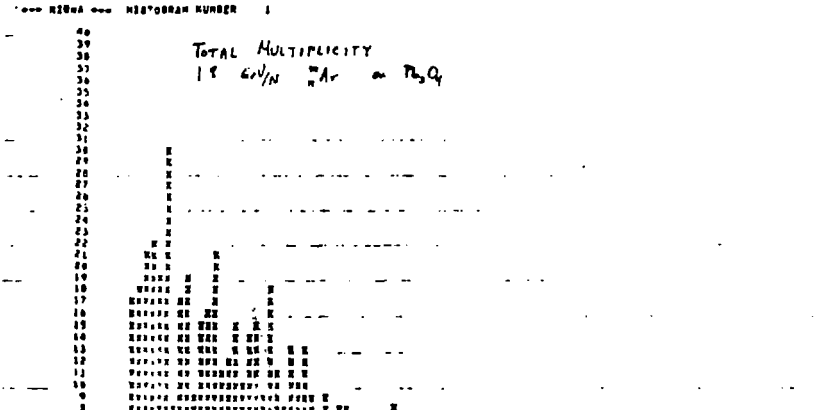

Fig. 25

These are multiplicity distributions from emulsions from the Heckman/Greiner group, for which they had defined central collisions to be those interactions for which there are no beam-like particles in a 5 degree cone. This distribution is much different from that of the streamer chamber, these being more symmetric and Gaussian-like.

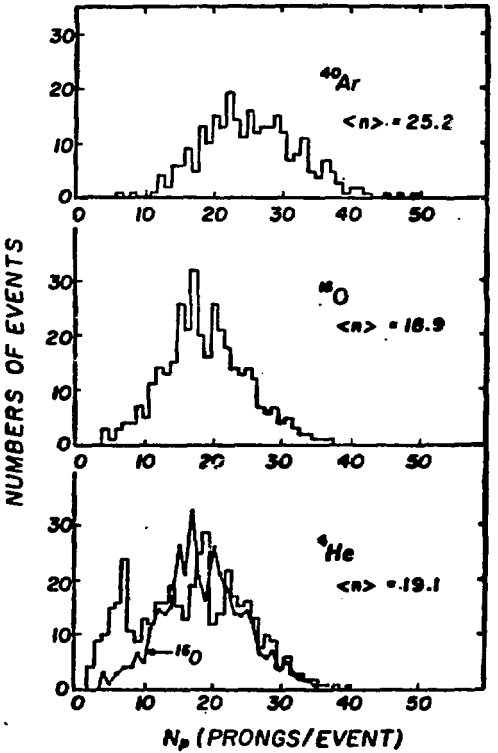

Fig. 26

We can compare those "unbiased" distributions with some that have been obtained triggered by particles at a finite angle, in this case, a fragment at 90 degrees. Again we see a sharply peaked distribution, not at all like the one from the streamer chamber. One has to understand what kind of bias this is.

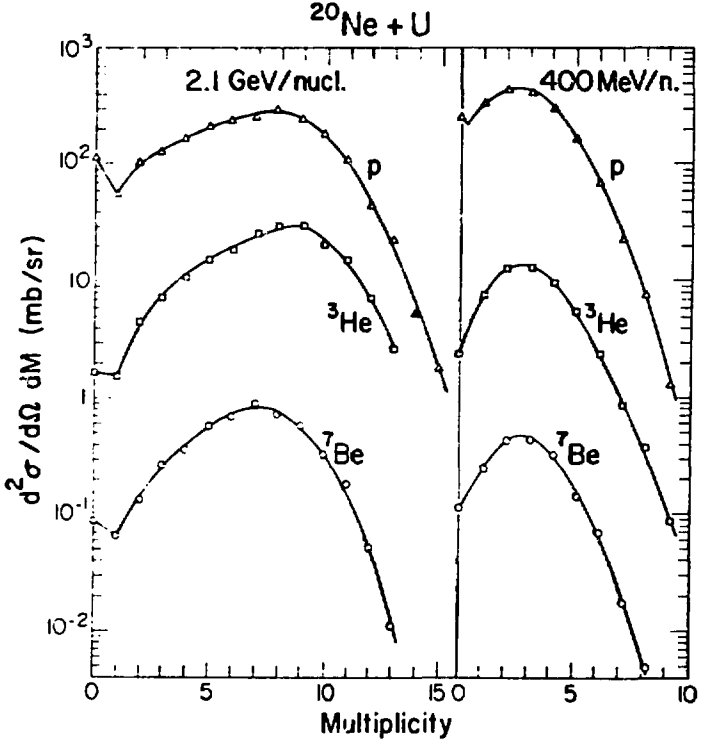

Fig. 27

Here we have plotted the mean multiplicities against a parameter, ⟨M⟩, which is essentially the average number of participants in a geometrical model. At 400 MeV/A the line has a 45 degree slope which means the mean multiplicity is equal to the amount of participants in the nucleus. At 1.05 GeV/A it is much higher than what the geometrical model would predict.

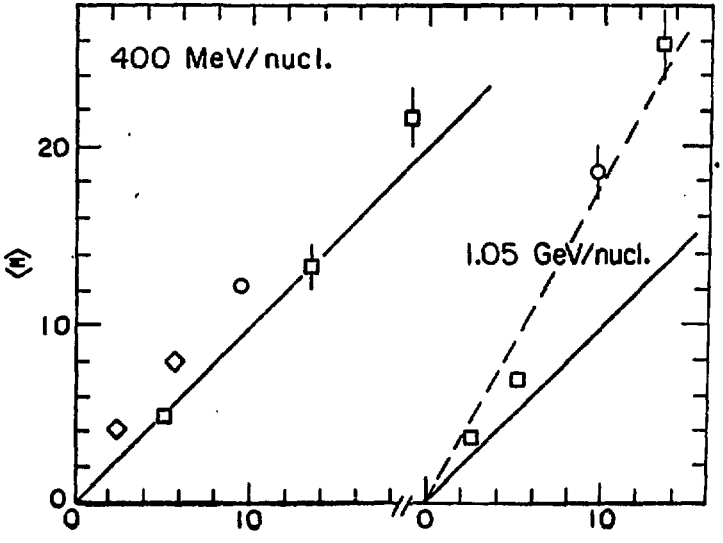

$$k = \frac{\pi r_0^2 \, (Z_t A_p^{2/3} + Z_p A_t^{2/3})}{\pi r_0^2 \, (A_p^{1/3} + A_t^{1/3})^2}$$

Fig. 28

Summary of Multiplicity Data:

a) Difficulty in defining a central collision (5, 10, 11)

b) Operational definition:

Central collisions are those in which there are no projectile remnants. (11)

c) The multiplicity shows a small dependence on the observed fragment. (4)

d) At 400 MeV/A the mean multiplicity <M> is equal to the mean number of participants in a geometrical model (clean cuts). (4, 5)

e) At 1.05 GeV/A <M> is twice as big.

Multiplicity Bias

Here we have for Ne on U at 3 energies the ratio of the cross section for high associated multiplicities to that for low multiplicities as a function of the laboratory angle of the telescope. You can see that there is a general trend of an increase in events with high multiplicities at backward angles.

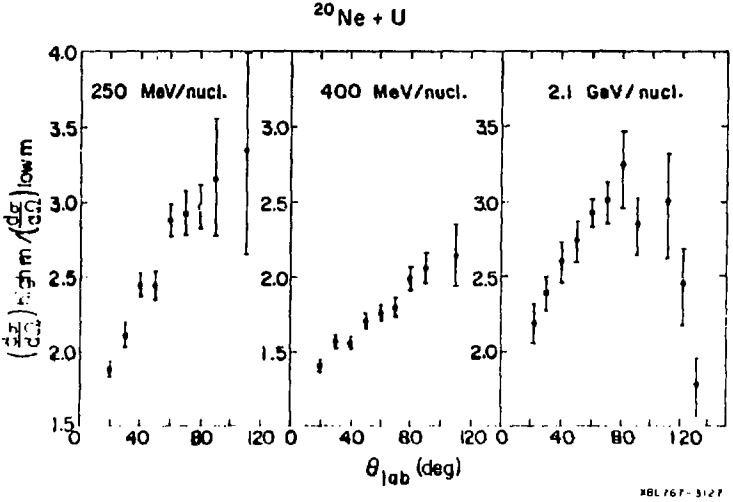

Fig. 29

A more dramatic bias on the multiplicity has been obtained in a measurement of the fission fragments we obtained from 400 MeV/A Ne on U and Au, shown here in a ΔE vs E plot. Shown are points corresponding to fission fragments and to fragments of mass from Ne up to Mg and higher.

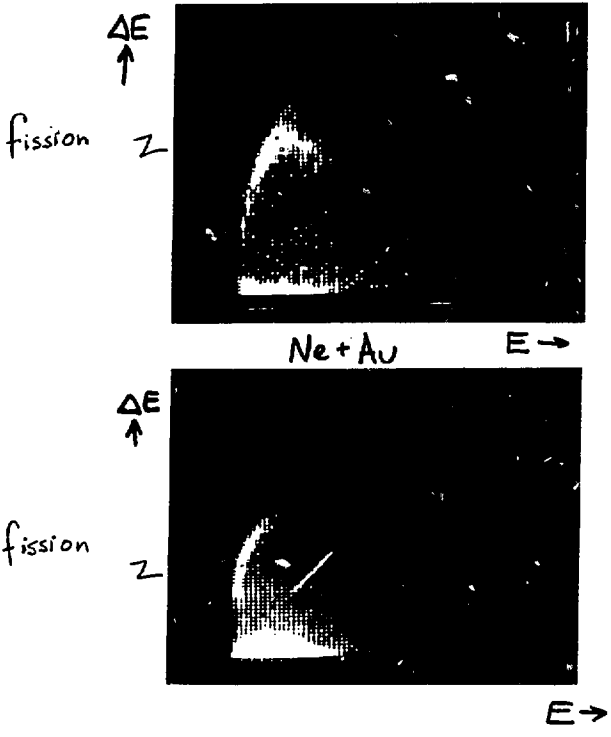

Fig. 30

The multiplicity distributions for these two components show a radical difference, that for the light fragments peaking at a multiplicity of around 12 and 14, while the fissioning channel has a very low multiplicity peaked at 0 for both targets.

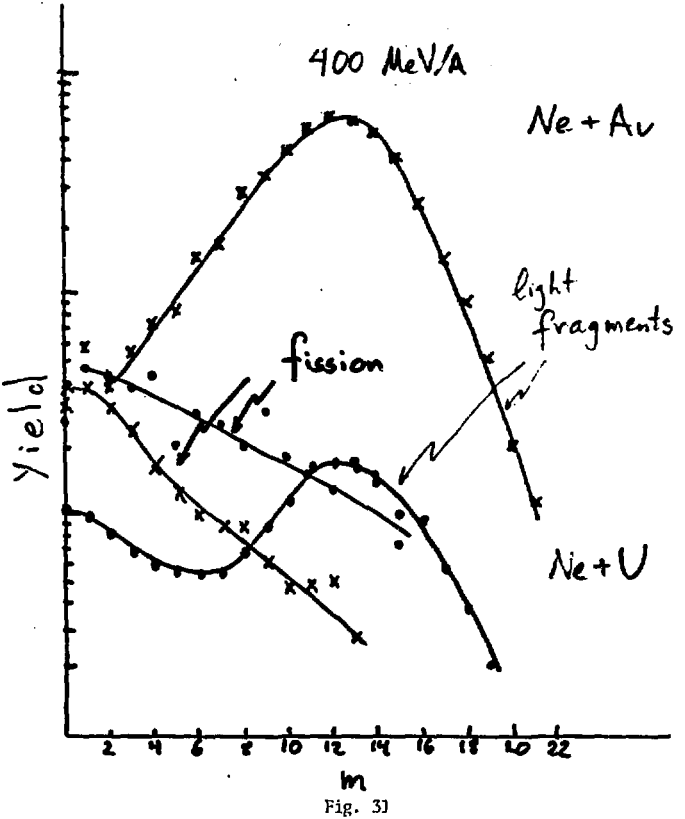

Fig. 31

Summary of the effects of biasing on different multiplicities:

a) Increased large angle emission for high multiplicity events (1, 4, 5)

b) The fission channel has a much lower multiplicity, corresponding to larger impact parameters. (19)

Correlations

We have been talking mainly about data that is being fit by thermal theories so it would be interesting to see the amount of thermalization taking place in these reactions.

These are data taken by Nagamiya, measuring a two particle correlation, namely the ratio of events for particles 180 degrees apart in plane to those 90 degrees apart out of plane for proton production from carbon on carbon and from carbon on lead. We see that for the C on C there is a strong correlation in which the peak corresponds exactly to the proton–proton elastic scattering. This isn't really surprising for the C on C interaction. For C on Pb there is not such an indication. Still this doesn't imply that those are equilibrated.

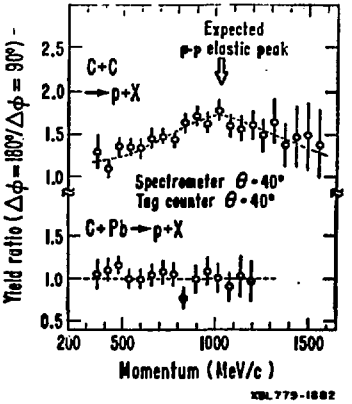

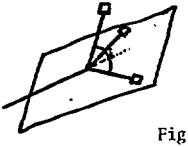

Fig. 32

A different type of correlation analysis was done by Jacquot for 15 emulsion stars with prong numbers varying between 7 and 30. A high multiplicity event, projected on the transverse plane is shown here.

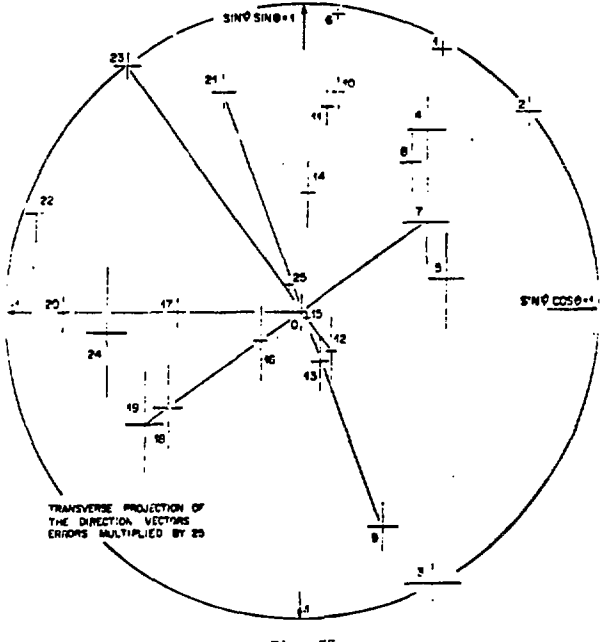

Fig. 73

He did a coplanarity analysis described below.

Jacquot

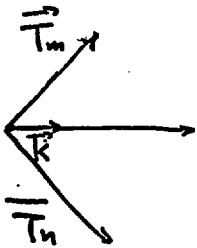

Fig. 34

Coplanarity analysis

Let $\vec{T}_m$ and $\vec{T}_n$ be the unit vectors along the direction of two tracks in an emulsion experiment.

Define

$B_{1,m,n} = \vec{k} \cdot (\vec{T}m \wedge \vec{T}n)$

with $\vec{k}$ the beam direction.

Two particles are coplanar if

$$|B_{1\ m,n}| \leq \Delta B_{1,m,n}$$

Construct

$$A = \sum_{m \neq n} e^{-\left(\frac{B_{1,m,n}}{\Delta B_{1,m,n}}\right)^2} .$$

To evaluate the probability of casual aligment distort each track by a $\Delta\phi$ random between $-\beta_{max} \leq \Delta\phi \leq \beta_{max}$

Such that there is not more than 250 MeV/c transverse momentum violation.

Construct A_{Random} with this distorted sample.

His results are shown here as a frequency histogram of the ratio of the coplanarityy coefficients for real to distorted events. They conclude that the deviations from the statistically expected distributions are significant but don't give any interpretation as to its meaning. They note, though, that for half of the coplanar tracks both lie on the same side of the beam axis.

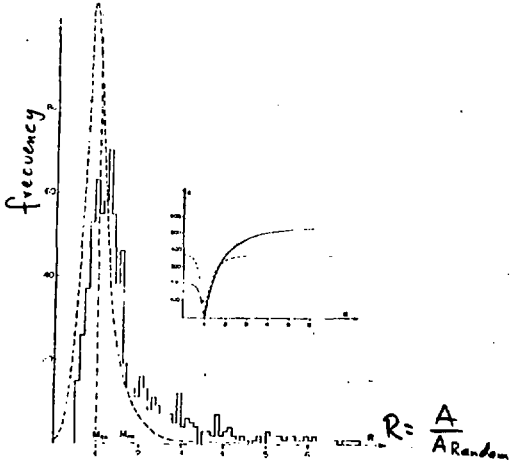

	EVENT n°	1	2	3	4	5	6	7	8	9	10	11	12	13	14	15
1	TOTAL MULTIPLICITY	30	26	26	13	14	11	11	12	8	9	9	7	10	10	7
2	3 prong Alignment	5	3	1	1	2		1		2	3			1	4	
3	4 prong Alignment	1	1	1	1	1	3	1	3			1	1	1	1	1
4	5 prong Alignment		1	1										1		
5	TOTAL prong Alignment	16	13	14	6	5	3	6	3	3	3	3	3	4	3	3
6	3 - prong (%) / N(%)	56 / 15	67 / 7	56 / 0	35 / 23	42 / 8	33 / 17	46 / 4	33 / 17	84 / 16	33 / 17	37 / 33	30 / 0	45 / 3	30 / 12	33 / 7

Fig. 35

Another correlation analysis was made by Chernov, again on emulsion stars. Measuring the emission angles, he constructed the standard correlation functions, C_2, R_2, and found very prominent structures. But he could reproduce them exactly with a Monte Carlo calculation, and concludes that there are no correlations besides phase space.

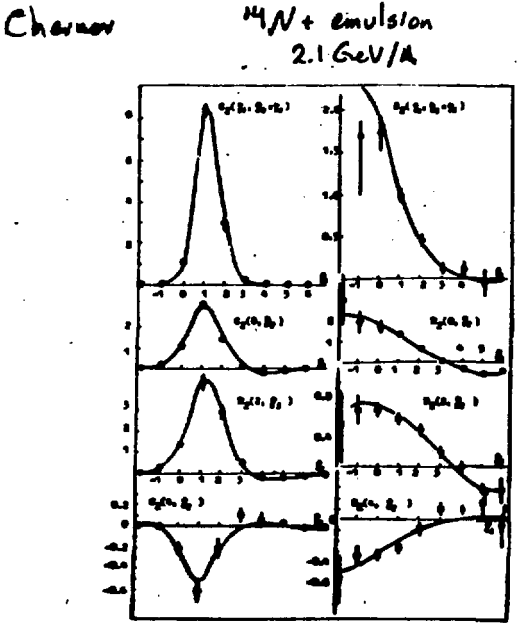

$$C_2(z_1, z_2) = \frac{1}{\sigma_{in}} \frac{d^2\sigma}{dz_1 dz_2} - \frac{1}{\sigma_{in}^2} \frac{d\sigma}{dz_1} \frac{d\sigma}{dz_2}$$

$$R_2(z_1, z_2) = \sigma_{in} \frac{d^2\sigma}{dz_1 dz_2} \Big/ \frac{d\sigma}{dz_1} \frac{d\sigma}{dz_2} - 1$$

Fig. 36

Summary of correlations:

a) Evidence for non thermalization on C + C. (1)

b) Contradictory results, probably due to the difficulty of defining what phase space and conservation laws would give as correlations. (11, 12, 15)

I will finish by summarizing some of the needs there are for data.

1. Data for trivial effects like $p + A \rightarrow$ π, p, ., ., . at the relevant bombarding energies.

2. To get a handle on the degree of equilibration
   a) in the fireball volume
   b) in the firestreak volume.

3. Theory that can analyze one single exclusive event:
   multiplicity
   baryon/meson
   nucleons/composites
   total $p_\perp$

4. Determine experimentally the mean free path for momentum degradation, which possibly can be extracted from Anderson's data
   $a \rightarrow$ H, C, Cu, Pb

5. For correlation studies be able to provide the quantities for uncorrelated events to compare to.

6. For comparison with theory the absolute cross sections are very important.

Requirements for the ideal central collision experiment to search for high density effects:

a) Equal projectile and target mass

b) No projectile–like fragments

c) Measurement of all momenta of produced particles exclusively.

d) A couple of good theoreticians.

Anderson

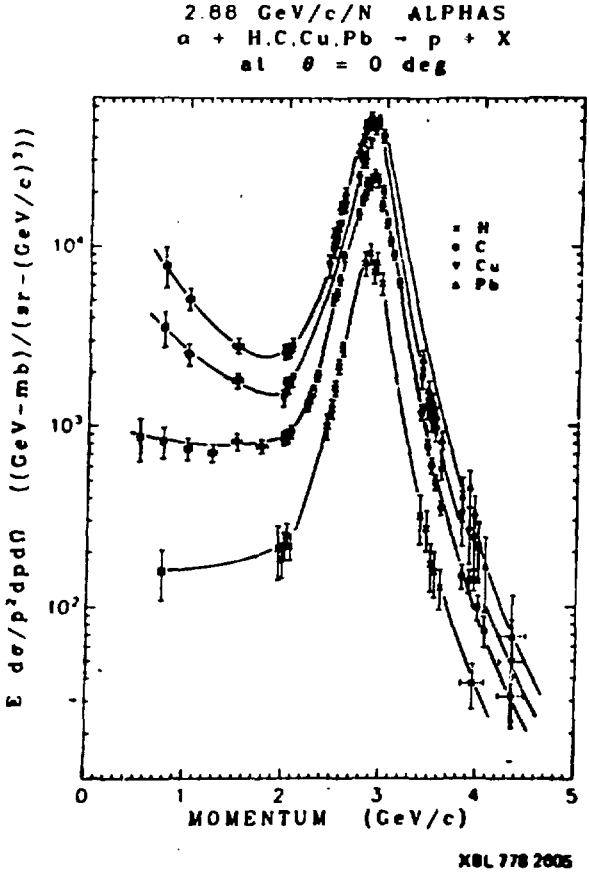

Fig. 37

COMPARISON OF MODELS OF HIGH ENERGY NUCLEAR COLLISIONS*

Miklos Gyulassy

I. Hopes and expectations

II. Choice of theoretical framework

III. The zoo of models (p inclusive)

IV. Light composites

V. Models vs. experiment
What have we learned?
What experiments are needed?

VI. Pion production

*(See LBL-6594 preprint)

I. Expectations, hopes, and goals of high energy heavy ion collisions.

A. For $E \gtrsim 100$ MeV/A, $V \approx V_{sound}$, $V_F \approx \frac{c}{4}$.

$\Rightarrow$ expect density pileups (shock waves)

$$\underline{\rho \sim (2 - 4)\,\rho_o} \quad , \qquad \rho_o = 0.17\ \mathrm{fm}^{-3}$$

Also expect high internal excitation energies $\underline{E^* \sim 50 - 100\ \mathrm{MeV/A}}$

$\therefore$ Extreme conditions $[\rho > \rho_o,\ E^* > E_F]$ far outside realm of conventional nuclear physics $[\rho \leq \rho_o,\ E^* \ll E_F]$

B. Hope is that novel collective phenomena will be observed:

*Density isomers (Lee, Wick; Greiner et al.)
*Pion condensation (Migdal; Sawyer; Baym, ...)
*Dynamic pionic instabilities (Gyulassy, Greiner, Ruck)
*Quark soup! (Chapline, Kerman)

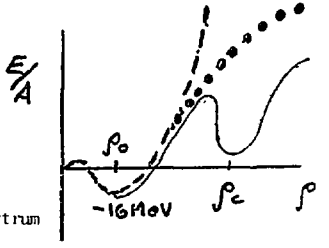

B'. Hope to learn about baryon spectrum (Glendenning, Karant)

C. Major goal of high energy heavy ion collision to learn about nuclear matter equation of state:

$$\underline{E/A \equiv W(\rho, T)}$$

Fig. 1

The determination of the nuclear incompressibility,

$$K \equiv 9\rho_0^2 \frac{\partial W}{\partial \rho^2} (\rho_0, 0),$$

would alone be a great achievement.

II. Which theoretical framework?

A. The ultimate theory should include

1. particle (π) production 2. quantum effects 3. nucleon interactions 4. many body correlations 5. finite geometry	Relativistic Quantum Field Theory: with explicit meson degrees of freedom

B. For $E \lesssim 500$ MeV/A, (1) can be neglected

RQFT → Quantum Many Body Theory with effective NN potentials

(Kauffmann is attempting to solve this)

C. Can we neglect quantum effects?

1. Interference: $\frac{2\pi\hbar}{\sqrt{2mE}} \sim$ 1-2fm $\approx \lambda = \frac{1}{\sigma\rho} \sim$ 2fm

Need a random phase assumption:
many collisions ⇒ loss of phase information

2. Off-shell: $\Delta E \sim \frac{\hbar V}{\lambda} \sim 50 - 100$ MeV

$\Rightarrow \frac{\Delta E}{E} \sim 25\%$ ⇒ can ≈ neglect off-shell

∴ For $100 \lesssim E \lesssim 500$ MeV/A, a <u>classical</u> framework has <u>partial</u> validity.

D. Classical Dynamics:

Equations of Motion with effective NN forces (Bodmer, Wilets)

Numerical complexity necessitates even further simplifications!

(We are getting further and further away from Paradise)

Heavy Ion time scales for 100 ~ 500 MeV/A:

1. τ_{int} = force range/c $\sim \frac{\hbar}{m_\pi c^2} \sim$ <u>1 - 2 fm/c</u>

2. $\tau_{rel} = \lambda/V \sim 3 - 4$ fm/c

3. $\tau_{col} = L/V \sim 10 - 20$ fm/c

$$\boxed{\tau_{int} < \tau_{rel} < \tau_{col}}$$

1. If $\tau_{int} \ll \tau_{rel} \Rightarrow$ isolated 2 body collisions (dilute gas limit)

   Eq. of Motion $\rightarrow$ { Boltzmann equation / Intranuclear cascade

2. If $\tau_{rel} \ll \tau_{col} \Rightarrow$ many collisions $\rightarrow$ thermalization

   Eq. of Motion $\rightarrow$ Hydrodynamics $W(\rho,T)$ is then input

3. If $\tau_{int} \ll \tau_{rel} \ll \tau_{col} \Rightarrow$ equilibrated dilute gas

   Eq. of Motion $\rightarrow$ Hydrodynamics with Ideal gas $W(\rho,T) = 3/2\ T$

*Note that none of these approximations can be rigorously justified for high energy heavy ion collisions but each is at least partially justified.

However, $\tau_{int} < \tau_{rel} < \tau_{col}$ implies that each is at least partially justified. The errors inherent in each approximation cannot be determined a priori.

MODELS OF HIGH ENERGY HEAVY ION COLLISIONS:

I. Macroscopic: Assume local thermal equilibrium

A. Ideal Gas $W(\rho,T)$ - no compression effects

1. "Fireball" - no T, $\tilde{v}$ gradients (Westfall, et al; LBL)
2. "Firestreak" - with T, $\tilde{v}$ gradients (Myers; LBL)

B. Realistic $W(\rho,T)$ - finite K ~ 300 MeV

3a. "1-fluid hydro" (Nix, Amsden, Harlow; LASL)

II. Semi-Microscopic: finite mean-free path

A. Continuum, partial equilibrium

3b. "2-fluids hydrodynamics" (Nix, et al., Goldhaber; LASL)

B. One dimensional cascade

4. "Row on Row" (Hüfner, Knoll; MPIM)

C. Knock-out (Koonin) (Blankenbeckler)

III. Microscopic: Input NN cross sections

A. Ideal classical cascade

5. "Hard spheres" (Halbert, et al.; OkNL)

B. Experimental cross section

6. "Cascade 1" - (Ginocchio; LASL)
7. "Cascade 2" - (Smith, Danos; Duke)
8. "Cascade 3" - (Fraenkel)

(IV. Quantal Many Body (Kauffmann))

Thermodynamic Models:

Assume: 1. $$f(\tilde{p},b) = \frac{1}{(2\pi mT(b))^{3/2}} \exp\left\{ - \frac{(\tilde{p}-\tilde{p}_{cm}(b))^2}{2mT(b)} \right\}$$

2. $p_{cm}(b)$ and $T(b)$ given by energy momentum conservation ($E^* = 3/2\ T$)

3. $$\frac{d^3\sigma}{dp^3}\ (A_p + A_T \to p + X) = \int_0^{R_p+R_T} 2\pi b db\ N(b)\ f(\tilde{p},b)$$

a) Fireball: (Westfall, et al., LBL)

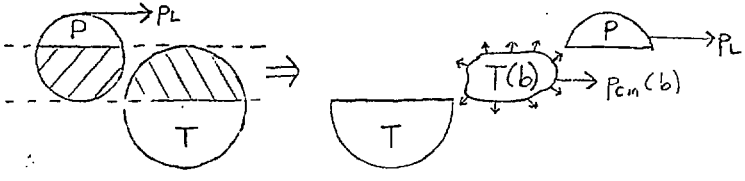

b) Firestreak: (Myers, LBL) (can include diffuseness)

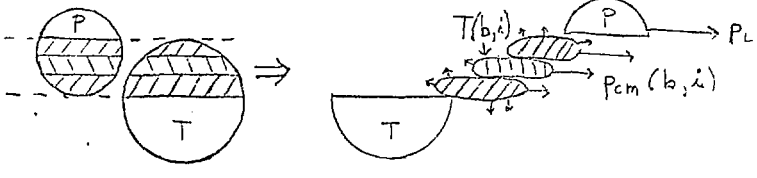

Fig. 2

Neglects
1. Compression effects
2. Spreading of interaction region $\perp$ to beam

3. Hydrodynamics (Nix, Amsden, Harlow)

Advantages:
1. $\tau_{rel} \ll \tau_{col}$ is a approximately satisfied
2. Deals directly with $W(\rho,T)$
3. Finite 3D geometry

*Neglects viscosity, dissipative effects even though

$$|\vec{\nabla}\rho| \not\ll \rho/\lambda \Rightarrow \text{ need Navier Stokes}$$

- Numerical reliability of computer code is difficult to assess.

a) 1-fluid model

$$\partial/\partial t \begin{pmatrix} \rho \\ \vec{m} \\ e \end{pmatrix} + \vec{\nabla} \begin{pmatrix} \vec{V}\rho \\ \vec{V}\vec{m} \\ \vec{V}e \end{pmatrix} = \begin{pmatrix} 0 \\ -\vec{\nabla}p \\ -\vec{\nabla}\cdot\vec{V}p \end{pmatrix} \Bigg\} \text{ Baryon momentum conservation energy}$$

Pressure: $p = \rho^2 \partial W(\rho,T)/\partial\rho|_{\text{const. entropy } S(\rho,T)}$

b) 2-fluids model:

- treat projectile and target as separate fluids
- interacting via energy momentum exchange:

$$\langle \dot{\vec{m}}_{P\to T} \rangle = [\rho_P \rho_T \sigma_{NN} |\vec{V}_P - \vec{V}_T|] \; [\alpha m(\vec{V}_P - \vec{V}_T)]$$

$$\approx 40 \text{ mb} \quad \alpha \approx (1/4 - 1/2)$$

Simulates partial transparency

Note on 1 - fluid pictures

1) Central collisions refractive effects due to finite geometry destroys Mach cone
2) Large perpendicular spreading of interaction region in contrast to fireball and streak
3) Striations indicate possible numerical instabilities at large b

Note on 2 - fluids model

1) Transparency
2) Slower perpendicular spreading of internal region

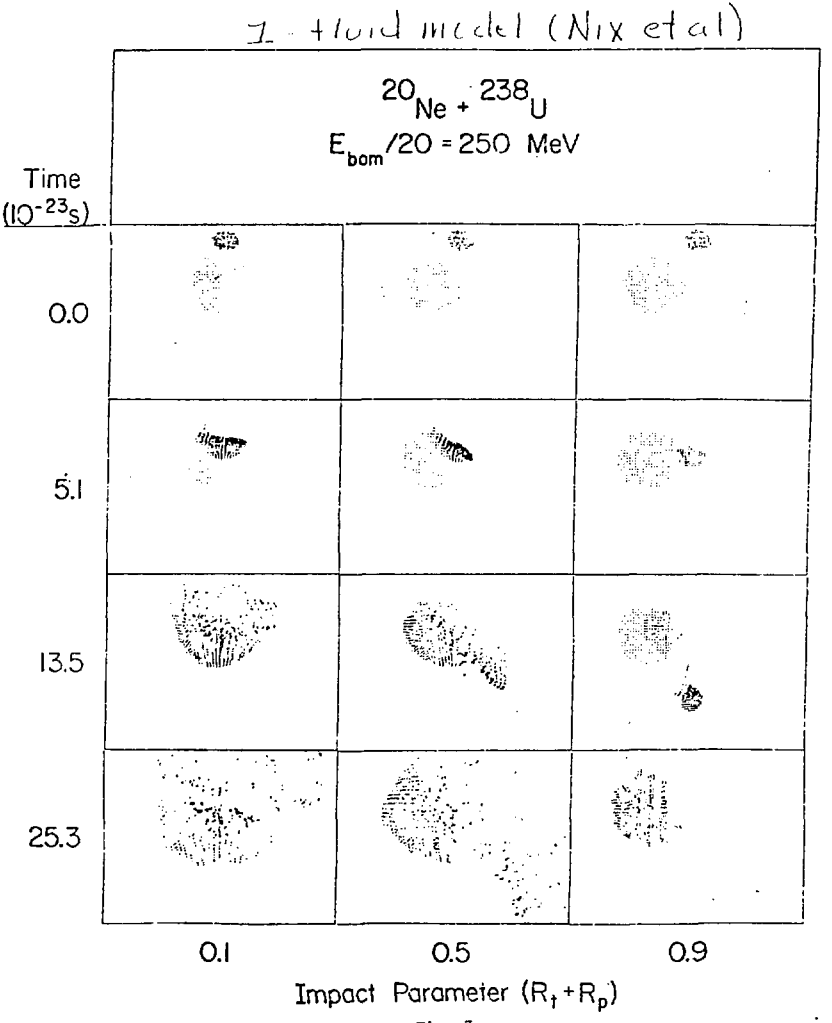
I - fluid model (Nix et al)
$^{20}Ne + ^{238}U$
$E_{bom}/20 = 250$ MeV
Time (10^{-23}s)
0.0
5.1
13.5
25.3
0.1
0.5
0.9
Impact Parameter ($R_t + R_p$)

Fig. 3

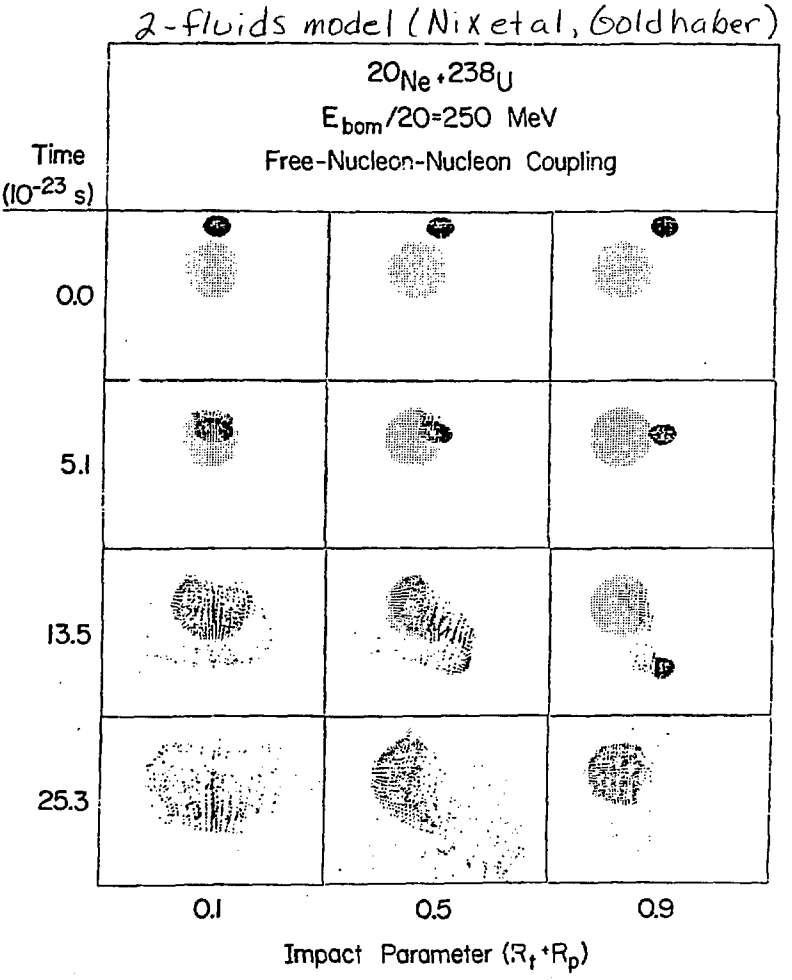
2-fluids model (Nix et al, Goldhaber)
$^{20}Ne + ^{238}U$
$E_{bom}/20 = 250$ MeV
Free-Nucleon-Nucleon Coupling
Time (10^{-23} s)
0.0
5.1
13.5
25.3
0.1
0.5
0.9
Impact Parameter ($R_t + R_p$)

Fig. 4

3) Yet final distribution rather similar to one fluid

→ insensitivity of results to non-equilibrium-dynamics

---

4. "Row on Row" (Hüfner and Knoll)
   Linear cascade ≈ semi-microscopic Firestreak

   Neglects 1. perpendicular spreading of cascade
   2. compression

A

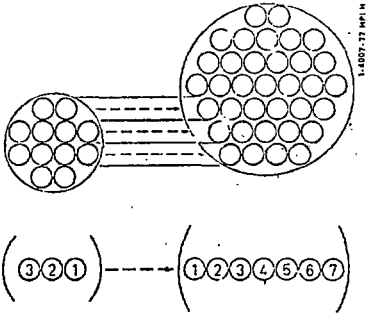

Fig. 5

Computes first two moments of each nucleon's momentum distribution via recursion relations.

longitudinal momentum distribution for 3 on 8

B

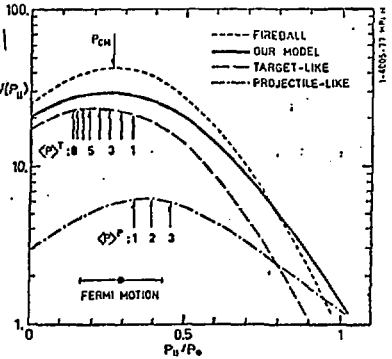

Fig. 6

"Quasi-Theorem":

If $\lambda_{stop} < L$, then central limit th. $\Rightarrow$ $f(\tilde{p}) = \frac{1}{(2\pi\sigma^2)^{3/2}} e^{-\frac{(\tilde{p}-\tilde{p}_o)^2}{2\sigma^2}}$

and energy, momentum conservation determine $\vec{p}_o$, σ^2.

5. "Hard Spheres" (Halbert et al.)
   Monte Carlo classical cascade with
   1. hard spheres $r = 0.45$ fm $\Rightarrow \sigma = 25$ mb
   2. soft spheres: for $b < 2r$, random 4π scattering at point of closest approach

$\therefore$ Both scattering mechanisms lead to ideal gas

$$W(\rho,T) = 3/2T \quad \text{for} \quad \rho \le \rho_c \approx 15\rho_o$$

Yet different pressures $P = \rho^2 \left.\frac{\partial W}{\partial \rho}\right|_S$!!

(e.g. $P \approx \frac{\rho T}{1-\rho/\rho_S}$ dilute hard sphere)

$$\therefore \rho_{max} \approx \begin{cases} 2\,\rho_o & \text{for hard spheres} \\ 4\,\rho_o & \text{for soft spheres} \end{cases}$$

Knowledge of $W(r,T)$ is *NOT* sufficient to determine the dynamics

This makes determination of W from heavy ion collisions very difficult!

6. Cascade 1 (Ginocchio)

Independent nucleon-nucleus cascade

$$A_P + A_T \xrightarrow{\text{approx.}} A_P \times (n + A_T)$$

use VEGAS code

- neglects collisions between cascading nucleons
- no density pileup
- optical potential absorb

$\Rightarrow$ too few NN collisions

Result: $d\sigma/d\Omega dE \sim \frac{1}{5}$ (experiment)

$\therefore A_P + A_T \neq A_P \quad (n + A_T)$!!

---

7. Cascade 2 (Smith, Danos)

Full 3D intranuclear cascade with π production, binding, fermi motion, surface, exclusion principle

- uses very novel numerical techniques
- very expensive
- not free from difficulties:
  1. $n + A_T$ data not reproduced
  2. other cascade model (Z. Fraenkel) on Ne + U gives different results.

However, great versatility of code allows study of effect of specific microscopic details on final results.
Also, phenomenal success for Ne + U $\rightarrow$ p + X.

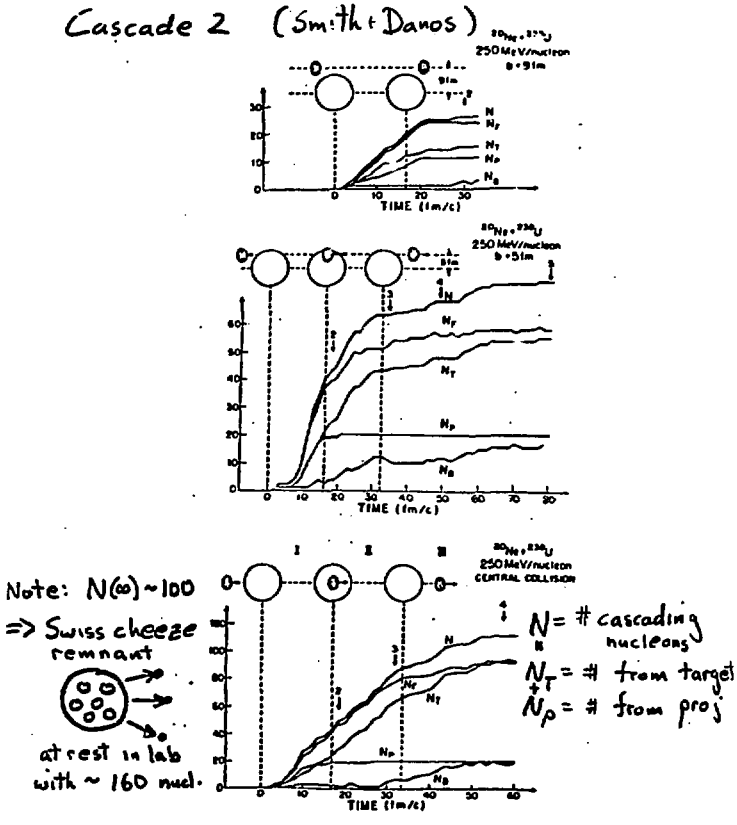
Cascade 2 (Smith + Danos)
250 MeV/nucleon
b = 9 fm
N
N_F
N_T
N_P
N_B
TIME (fm/c)
250 MeV/nucleon
b = 5 fm
250 MeV/nucleon
CENTRAL COLLISION
Note: N(∞) ~ 100
=> Swiss cheeze remnant
at rest in lab with ~ 160 nucl.
N = # cascading nucleons
N_T = # from target
N_P = # from proj

Fig. 7

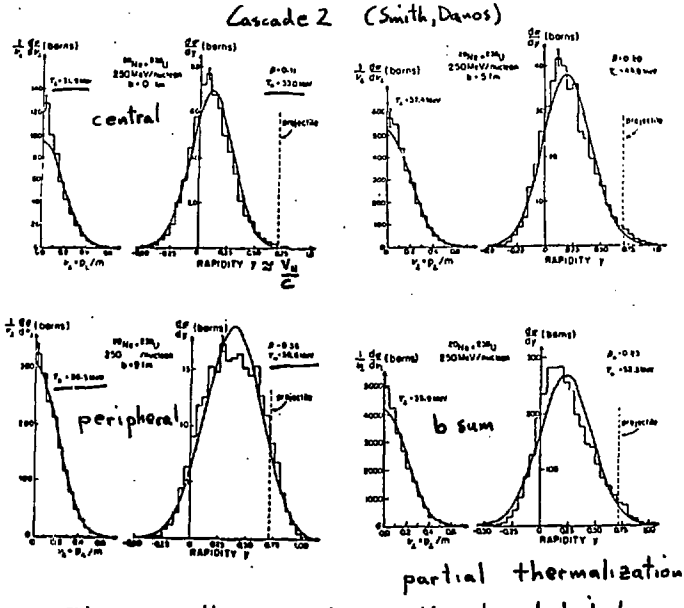

These results are not sensitive to detailed NN scatt cross sec.

Fig. 8

IV. Light Composites

Experiment:

for $E_{lab} \lesssim 50$ MeV/nuc., up to 70% of nucleons emerge in light Fragments: d, t, He, ...

1) Coalescence Model (Johansen, et al.)

$$\frac{d^3\sigma(A)}{dp^3} \propto \left(\frac{d^3\sigma(p)}{dp^2}\right)^A (p_o)^{3A-3}$$

where $p_o(d)$, $p_o(t)$, ... $\approx 100 - 140$ MeV/c

define coalescence radii in phase space
(relation verified experimentally)

2) Chemical Equilibrium (Mekjian)

assume existence of source with β,T

$$\frac{d^3\sigma(A)}{dp_{cm}^3} \propto e^{-E_{tot}/T} \propto \left[e^{-(E_t/A)/T}\right]^A \propto \left(\frac{d^3\sigma(p)}{dp_{cm}^3}\right)^A$$

* Same relation as in (1)

Normalization follows from law of mass action

$$\frac{\mathcal{N}(Z,N)}{\mathcal{N}(p)^Z \mathcal{N}(n)^N} \propto \left(\frac{\lambda_T^3}{V_{freeze}}\right)^{A-1}$$

V_{freeze}: $R_f = \lambda(\rho_f) = \frac{1}{\sigma_{abs}^A \rho_f} \Rightarrow \rho_f \propto \left(\frac{1}{\sigma_{abs}^A}\right)^{3/2}$

$\Rightarrow$ mean free path
for absorbtion = size of system

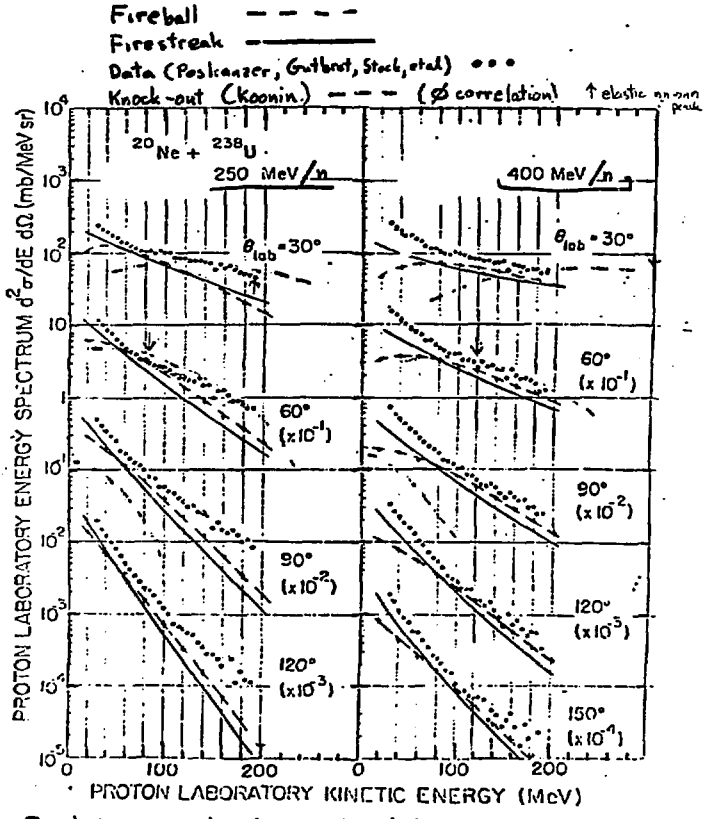

∴ Fireball ≈ Firestreak ≈ ½ data

because of ∫bdb because of neglect ⊥ spreading ?

Fig. 9

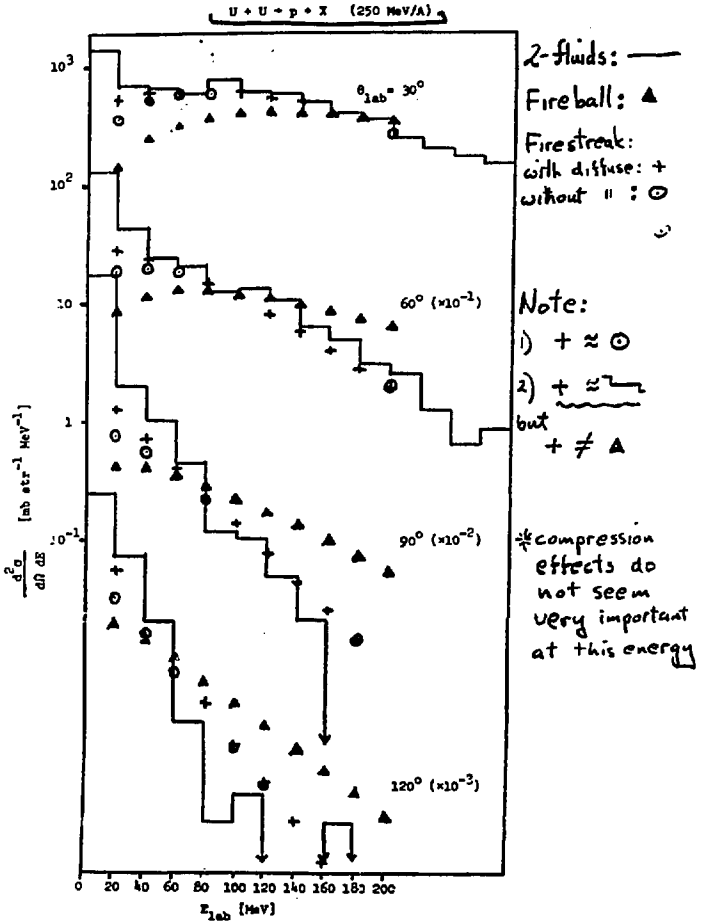
U + U → p + X (250 MeV/A)
2-fluids: ——
Fireball: ▲
Firestreak:
with diffuse: +
without " : ⊙
Note:
1) + ≈ ⊙
2) + ≈
but
+ ≠ ▲
*compression effects do not seem very important at this energy
θlab = 30°
60° (×10⁻¹)
90° (×10⁻²)
120° (×10⁻³)
d²σ/dΩ dE [mb str⁻¹ MeV⁻¹]
Elab [MeV]
0 20 40 60 80 100 120 140 160 180 200

Fig. 10

1. Hard spheres ≈ 1-fluid hydro ⇒ insensitive to $W(\rho,T)$
2. Cascade 1 ~ 1/3 data ⇒ $A_p + A_T \neq A_p(n+A_T)$

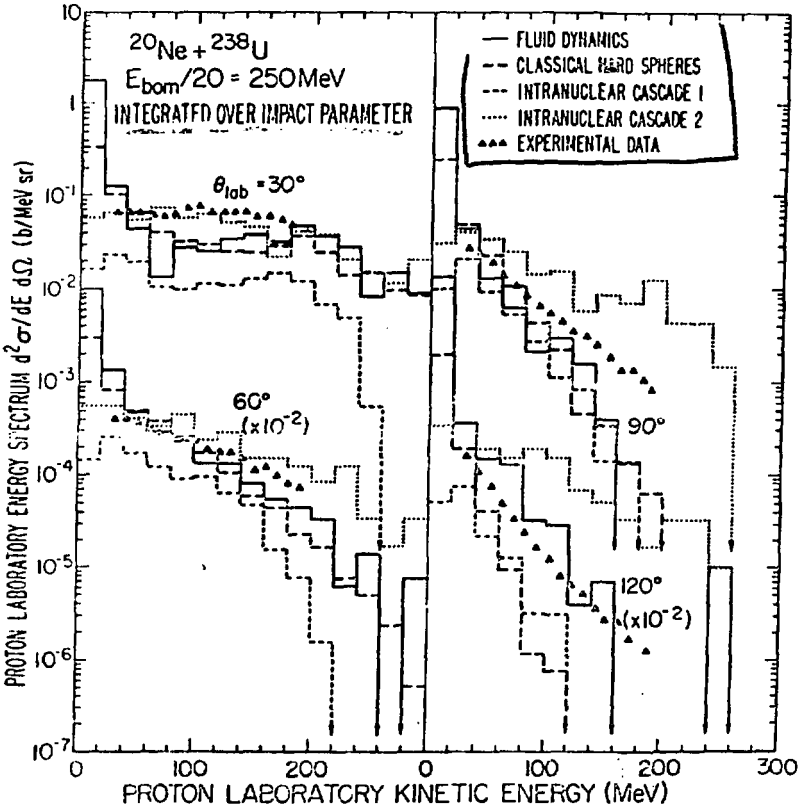

Fig. 11

∴b=0 results are much more sensitive to differences between models

Hard sph. (b=0) ≠ hydro (b=0)

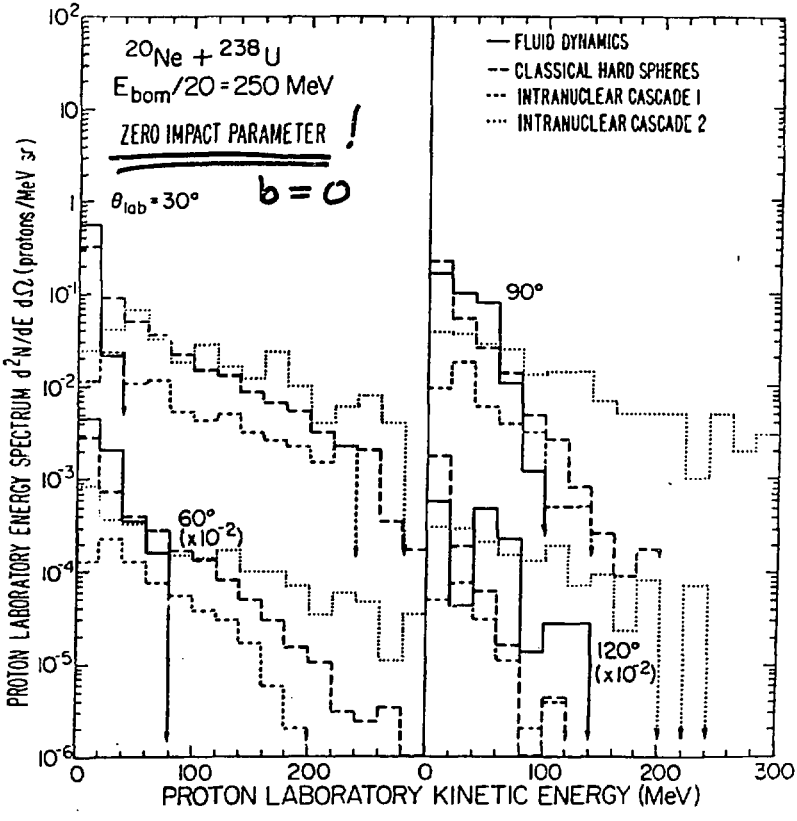

Fig. 12

LA-UR-77-2691, A.A. Amsden et al. two-fluid

U + U → p + X 2.1 GeV/A

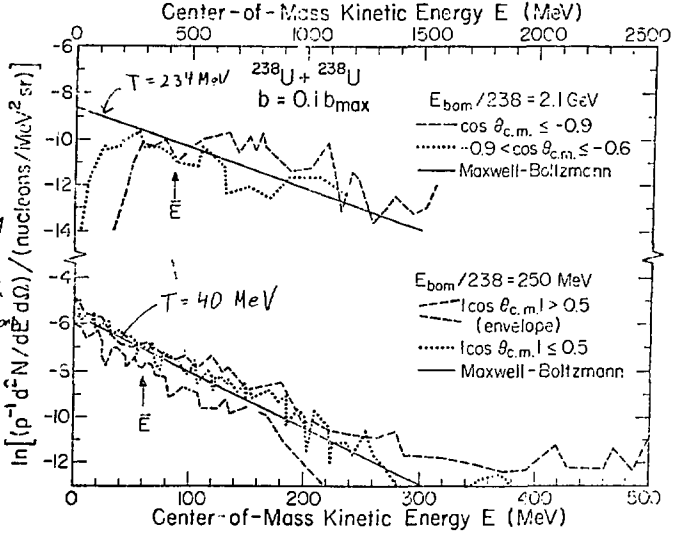

Note hole $E_{cm} < 200$ MeV at 2.1 GeV/A, could be due to explosion not seen in 250 MeV/A because of much lower compression at low energy]

Fig. 13

1 - fluids: —
2 - fluids: —

Nix. et. al.

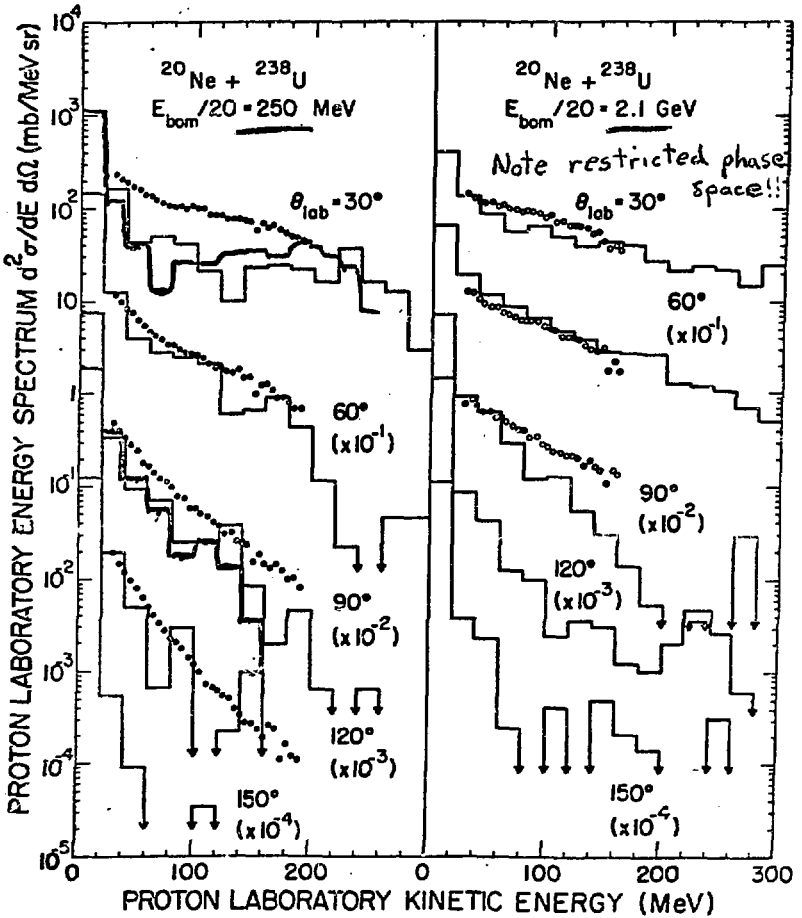

∴ summed results are not sensitive to non-equilibrium stage

Fig. 14

— Cascade 2 (Smith + Danos)

..... Z. Fraenkel "Cascade 3"

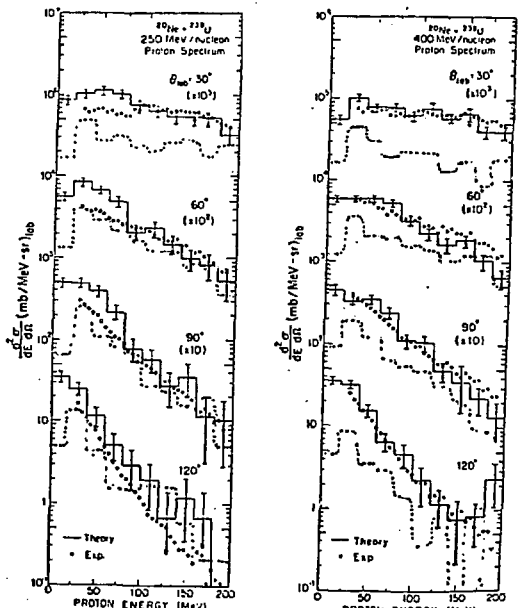

Will agreement remain after existing bugs in Cascade2 are eliminated?

Why do Cascade 2 + 3 differ??

Fig. 15

Thus, freeze-out density differs for all fragments!

F	d	t	He^3	He^4
ρ_f/ρ_o	0.25	0.40	0.40	0.67

(Mekjian)

Also, $T(\rho_f)$ is an unknown parameter

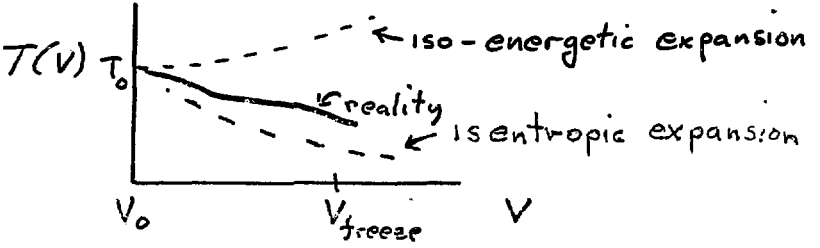

Fig. 16

∴ Taking $T(\rho_f)$ from iso-energetic curve and fixing ρ_f for all fragments to be the same cannot be justified (beware firstreakers)

Summary: proton + composite inclusive

1) ∃ *NO* theory of nuclear collisions
2) ∃ *PLENTY!* of models (classical)
3) Most models reproduce single particle inclusive data to factor ~ 2-4 because
   a) $\int bdb$ averages over errors
   b) $\lambda_{stop} < L \Rightarrow$ quasi-thermalization (insensitive to non-equilibrium details)
   c) correlation information averaged out in single particle observables

4) Differences between models is largest for $b \approx 0$ ⇒ must isolate

$b \approx 0$ collisions experimentally

$$A + A \to F + X \Big\} \begin{array}{l}\text{high multiplicity} \\ \text{+ azimuthal symmetry}\end{array}$$

5) Yet even for $b \approx 0$, $W(\rho,T)$ cannot be deduced from data (need $S(\rho,T)$ also)

Too bad Mach cones not observed!

Perhaps from explosion hole in $d^2\sigma/d\Omega dE$ relative stiffness can be found.

6) Azimuthal correlations can distinguish between knock-on and thermal models

⇒ need two particle inclusive, especially at high energy phase space (especially at the energy region above the proton-proton elastic peak)

VI. Pion production

Experiments:

1) $E^{cm} \lesssim 50$ MeV, isotropic
2) 50 ~ 200 MeV, anisotropic
3) $\gtrsim$ 200 MeV, isotropic

Models:

A. Independent $p + A \to \pi$ (Nakai)

$$d\sigma(A_p + A_T \to \pi) = Z_p\, d\sigma(p + A_T \to \pi) + N_p d\sigma(n + A_T \to \pi)$$

B. Chemical equilib π (Kapusta)

self consistent, chemically equilibrated, diffuse firestreak with *ONE* ρ_f

and $T(\rho_f)$ taken from iso-energetic expansion

- both (A) and (B) consistent with (1) to factor 2
- (A) consistent with (2); (B) *NOT* consistent (reasons: Δ_{33} production mechanism)

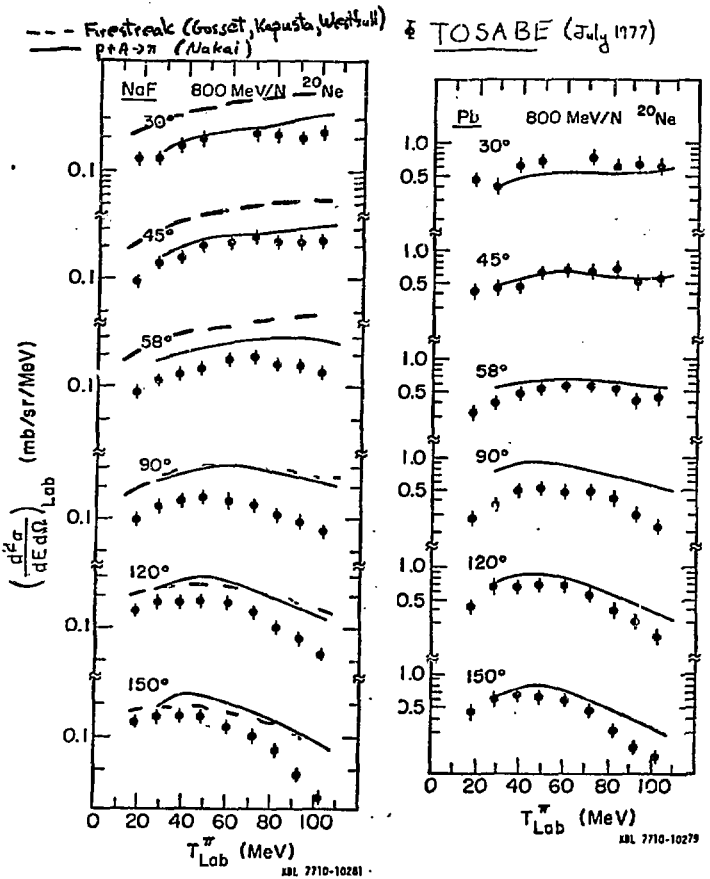
Firestreak (Gosset, Kapusta, Westfall)
p+A→π (Nakai)
TOSABE (July 1977)
NaF 800 MeV/N 20Ne
Pb 800 MeV/N 20Ne
30°
45°
58°
90°
120°
150°
0.1
1.0
0.5
(mb/sr/MeV)
$\left(\frac{d^2\sigma}{dE\,d\Omega}\right)_{Lab}$
0 20 40 60 80 100
T^{π}_{Lab} (MeV)
XBL 7710-10281
XBL 7710-10279

Fig. 17

Pion Multiplicity Distributions $\left\{ \begin{array}{l} Ar + Pb_3O_4 \rightarrow n \times \pi^-,\ 1.8\ GeV/A \\ \text{Poe et al}: \ \Phi \end{array} \right.$

Note: no copious π prod.

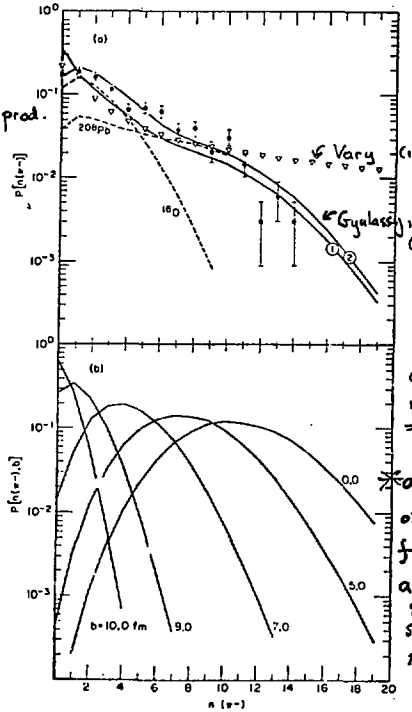

(independent coll. model)

(thermodynamic model)

absence of multipion correlations $\Rightarrow P(n,b) = \text{Poisson}$

$\Rightarrow$ any deviations of $P(n, b=0)$ from Poisson are truly significant signal of exotic π prod. mech.

Need $A + A \rightarrow n\pi^-]_{b=0}$ experimentally !

$\rightarrow$ If $P(n,0)$ is Poisson, then single π incl. contains more info.

Fig. 18

- (B) too high in region (3)

  reason: different mechanism = Fermi tail production?

  can be tested in $p + A \to \pi$(high energy)

  $\Rightarrow$ need such experiments

  (A) has not been tested in this region because

Summary of experiments needed soon to help weed out models:

- Single particle inclusive

  1) $A + A \to p, d, \ldots$ at $b \approx 0$

  2) $p + A \to$ high energy $\{^{\pi}_{p}\}$

- Two particle inclusive

  3) Azimuthal correlations between high energy fragments

- Multiparticle

  4) $A + A \to n \times \pi^-$ at $b \approx 0$

(Please, no more impact parameter averaged data).